

AD _____

Award Number: W81XWH-07-1-0128

TITLE: The Role of Membrane-Derived Second Messengers and Bmx/Etk in Response to Radiation Treatment of Prostate Cancer

PRINCIPAL INVESTIGATOR: Christopher Willey, M.D., Ph.D.

CONTRACTING ORGANIZATION: Vanderbilt University Medical Center
Nashville, TN 37232-5671

REPORT DATE: January 2009

TYPE OF REPORT: Annual Summary

PREPARED FOR: U.S. Army Medical Research and Materiel Command
Fort Detrick, Maryland 21702-5012

DISTRIBUTION STATEMENT: Approved for Public Release;
Distribution Unlimited

The views, opinions and/or findings contained in this report are those of the author(s) and should not be construed as an official Department of the Army position, policy or decision unless so designated by other documentation.

REPORT DOCUMENTATION PAGE				Form Approved OMB No. 0704-0188	
Public reporting burden for this collection of information is estimated to average 1 hour per response, including the time for reviewing instructions, searching existing data sources, gathering and maintaining the data needed, and completing and reviewing this collection of information. Send comments regarding this burden estimate or any other aspect of this collection of information, including suggestions for reducing this burden to Department of Defense, Washington Headquarters Services, Directorate for Information Operations and Reports (0704-0188), 1215 Jefferson Davis Highway, Suite 1204, Arlington, VA 22202-4302. Respondents should be aware that notwithstanding any other provision of law, no person shall be subject to any penalty for failing to comply with a collection of information if it does not display a currently valid OMB control number. PLEASE DO NOT RETURN YOUR FORM TO THE ABOVE ADDRESS.					
1. REPORT DATE 01-01-2009		2. REPORT TYPE Annual Summary		3. DATES COVERED 1 JAN 2007 - 31 DEC 2008	
4. TITLE AND SUBTITLE The Role of Membrane-Derived Second Messengers and Bmx/Etk in Response to Radiation Treatment of Prostate Cancer				5a. CONTRACT NUMBER	
				5b. GRANT NUMBER W81XWH-07-1-0128	
				5c. PROGRAM ELEMENT NUMBER	
6. AUTHOR(S) Christopher Willey, M.D., Ph.D. Email: christopher.willey@vanderbilt.edu				5d. PROJECT NUMBER	
				5e. TASK NUMBER	
				5f. WORK UNIT NUMBER	
7. PERFORMING ORGANIZATION NAME(S) AND ADDRESS(ES) Vanderbilt University Medical Center Nashville, TN 37232-5671				8. PERFORMING ORGANIZATION REPORT NUMBER	
9. SPONSORING / MONITORING AGENCY NAME(S) AND ADDRESS(ES) U.S. Army Medical Research and Materiel Command Fort Detrick, Maryland 21702-5012				10. SPONSOR/MONITOR'S ACRONYM(S)	
				11. SPONSOR/MONITOR'S REPORT NUMBER(S)	
12. DISTRIBUTION / AVAILABILITY STATEMENT Approved for Public Release; Distribution Unlimited					
13. SUPPLEMENTARY NOTES					
14. ABSTRACT Radiation-induced activation of the PI3K/Akt signal transduction pathway requires Akt binding to phosphatidyl-inositol phosphates (PIPs) on the cell membrane. The tyrosine kinase, bone marrow X-kinase (Bmx), binds to PIPs in a manner similar to Akt. Since Bmx is known to be involved in cell growth and survival pathways, Bmx could contribute to the radiation response within the vascular endothelium and prostate cancer, which highly express this protein. We therefore are studying Bmx signaling within the vascular endothelium and prostate cancer. Our initial studies have focused on the vascular endothelium. Bmx was activated rapidly in response to clinically relevant doses of ionizing radiation. Bmx inhibition enhanced the efficacy of radiotherapy in endothelial cells (human umbilical vein endothelial cells or HUVEC) within in vitro systems. Retroviral shRNA knockdown of Bmx protein enhanced HUVEC radiosensitization. Furthermore, pretreatment of HUVEC with a pharmacological inhibitor of Bmx, LFM-A13, produced significant radiosensitization of endothelial cells as measured by clonogenic survival analysis and apoptosis as well as functional assays including cell migration and tubule formation. In vivo, LFM-A13, when combined with radiation resulted in significant inhibition of blood flow within prostate tumors as measured by pixel weighted power doppler. However, when tumor growth delay studies were performed in mice using human prostate cancers, the combination of LFM-A13 with radiation was not superior to either treatment alone. So, although LFM-A13 inhibition of Bmx did produce a tumor growth delay effect vs. vehicle control, no radiation enhancement was detected. Bmx, thus, represents a standalone molecular target for prostate cancer treatment and for radiosensitizing tumor vasculature, but how to best combine these treatments remains unclear.					
15. SUBJECT TERMS Prostate cancer, Bmx, tyrosine kinase, kinase inhibitors, angiogenesis, tumor vasculature, radiation					
16. SECURITY CLASSIFICATION OF:			17. LIMITATION OF ABSTRACT UU	18. NUMBER OF PAGES 25	19a. NAME OF RESPONSIBLE PERSON USAMRMC
a. REPORT U	b. ABSTRACT U	c. THIS PAGE U			19b. TELEPHONE NUMBER (include area code)

Table of Contents

	<u>Page</u>
Introduction.....	4
Body.....	4
Key Research Accomplishments.....	14
Reportable Outcomes.....	14
Conclusion.....	14
References.....	16
Appendices.....	16

INTRODUCTION

Patients with intermediate to high risk prostate cancer have a 30% risk of local recurrence despite receiving radiation. Hormone ablative treatment can improve the outcome including survival, especially when combined with regional radiation coverage. This suggests that the biological modification by hormone deprivation sensitizes the prostate cancer cells to radiation. In addition, dose escalation has been shown in a phase III trial to result in improved tumor control which further emphasizes the potential for improving outcomes by optimizing local control of prostate cancer.¹ Therefore, this new strategy to sensitize prostate cancer to radiation treatment is likely to translate into a significant survival benefit for patients afflicted with this disease. The tumor microvasculature is also a target for prostate cancer treatment.²⁻⁴ Both clinical and basic science research have identified the tumor microvasculature as a major factor that supports tumor growth. Moreover, this microvasculature is thought to contribute to the radiation resistance seen in many solid tumors. In order to improve outcomes, efforts aimed at improving local control through targeting of tumor vasculature have been undertaken. Our laboratory has studied the inherent resistance of the tumor vascular endothelium to the cytotoxic effects of IR. We have found that IR induces the activation of Bmx which regulates endothelial cell viability and function. Our preliminary studies show that radiation induces Bmx activation in a similar time course to PI3K/Akt activation and that a small molecule inhibitor of Bmx modulates the cellular viability of endothelial and prostate cancer cells, particularly with radiation. The goals of the proposed research study are to determine whether Bmx inhibition can enhance the cytotoxic effects of radiation in these endothelial and prostate cancer cells as well as to identify the mechanism by which Bmx is activated by radiation. Because this is the first description of Bmx activation by radiation, this research will potentially lead to a new molecular target for radiation sensitization. Our ultimate goal is to bring this therapeutic strategy into clinical trials.

BODY

Statement of Work - Examining Bmx within prostate cancer and tumor vasculature

Task 1. To determine the activation profile of Bmx in response to radiation in endothelial and prostate cancer cells and determine if Bmx inhibition can enhance radiation efficacy in these cells (Months 1-14):

The goal of this task is to characterize Bmx within *in vitro* model systems of both prostate cancer and vascular endothelium. The bulk of the work thus far has been performed within human umbilical vein endothelial cells (HUVEC) which are a model of the vasculature. One of the advantages of HUVEC is that they are pooled primary cultured cells from several human donors. As such, significant findings in these cells are more likely to have broad application for patients due to the heterogeneity. We have already accomplished most of the objectives that were proposed for this task, though we still need to test the prostate cancer cell lines using the same techniques.

a) Immunoprecipitate Bmx from irradiated endothelial cells and prostate cancer cells lines and assay them for kinase activity (Months 1-6).

Bmx is activated in endothelium upon irradiation

We examined primary culture vascular endothelial cells (HUVEC) to determine whether Bmx was activated by ionizing radiation, because of its similarities in structure and signaling with that of Akt, and was possibly contributing to radiation resistance. Figure 1A demonstrates a time course of Bmx activation upon irradiation with a clinically relevant dose of 2 Gy. Tyrosine 40, present in the PH domain of Bmx, becomes phosphorylated during its activation⁵. Bmx is phosphorylated at 60 min. following 2 Gy of irradiation. To confirm this finding, we utilized an *in vitro* kinase (IVK) assay in which Bmx was immunoprecipitated from irradiated or sham irradiated endothelial cells and then incubated with ATP in a kinase reaction. These samples were then run on SDS-PAGE and probed for anti-phosphotyrosine to analyze autophosphorylation of Bmx. As shown in figure 1B, Bmx was activated after irradiation. Examination of total Bmx revealed no change in Bmx levels at any of the time points that were assayed. Densitometric quantitation (mean and standard errors) from four separate experiments is shown as well. Interestingly, Bmx showed significant kinase activity immediately following irradiation and then has a second peak of lesser activity at 1h.

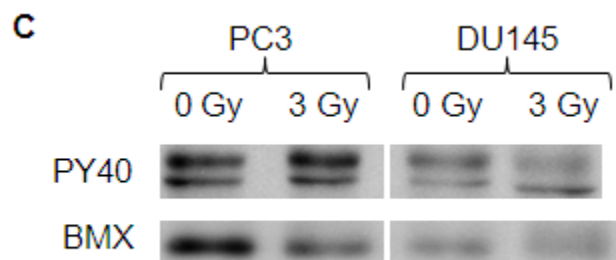
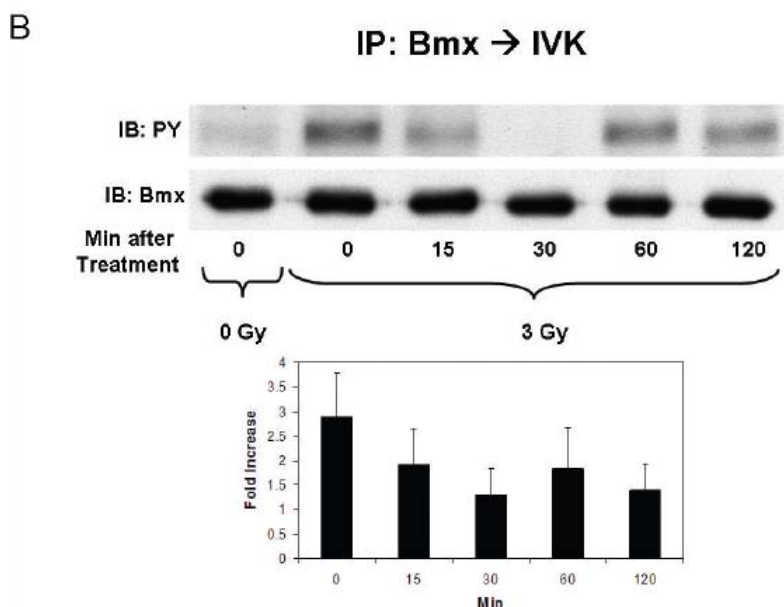
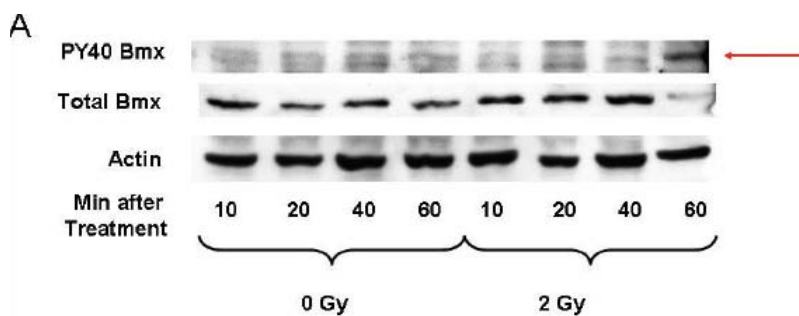


Figure 1. Bmx is activated by radiation in endothelial cells but is constitutively active in prostate cancer cells. Human umbilical vein endothelial cells (HUVEC) were either sham irradiated or radiated with 2 Gy. **A)** Cells were harvested and total lysates were made after incubation at 37° C for the indicated times in min. Western blots are shown of phosphotyrosine 40 (PY40) Bmx, indicative of activation, as well as total Bmx and actin for normalization. **B)** *In vitro* kinase assay (IVK). Bmx was immunoprecipitated (IP:Bmx) from the lysates and eluted under non-denaturing conditions. Following elution, kinase assay buffer was added for 20 min. Samples were separated by SDS-PAGE. Western blot analysis using anti-phosphotyrosine (IB:PY) antibody was used to detect autophosphorylation. Total Bmx levels are also shown (IB:Bmx) using anti-Bmx antibody. Densitometric quantitation of autophosphorylation was performed (n=4) and plotted as mean fold increase over 0 Gy conditions with standard errors shown. **C)** PC3 and DU145 human derived prostate cancer cells were either sham irradiated (0 Gy) or irradiated with 3 Gy. Cells were incubated for 30 minutes and then were harvested and prepared as total cell lysates. Western blots for total (BMX) and phosphorylated Bmx on Tyrosine 40 are shown.

Bmx is constitutively active in prostate cancer cells

We also examined PC3 and DU145 human prostate cancer cells for Bmx expression and activation. As shown in Figure 1C, Bmx is not only expressed but shows significant constitutive activation based on the level of phosphorylation of tyrosine 40. Because of this constitutive activation, we did not appreciate any significant increase in activation with 3 Gy.

b) Construct shRNA retrovirus vectors specific for Bmx, express them in endothelial cells, and assay endothelial cell function with radiation (Months 1-12).

Bmx knockdown enhances radiation efficacy in endothelium

Because we were able to detect a clear activation of Bmx following a clinically relevant dose of IR, we wanted to determine whether Bmx activation protects the endothelial cells from cytotoxic damage. Since primary culture endothelial cells, such as HUVEC, have low transfection yields, we utilized a retroviral shRNA system to knockdown Bmx levels prior to irradiation. Figure 2A shows five different retroviral constructs (A through E) for Bmx as well as a negative control construct (Neg) that were used to infect HUVEC. After 48 h, infected cells

were harvested and lysates were prepared for total Bmx Western blotting. As can be seen, construct A (shBmxA) provided ~90% knockdown of Bmx protein levels compared to the negative control shRNA vector. Bmx knockdown experiments were performed with or without irradiation. Figure 2B shows MTT-based (WST-1) survival assay. HUVEC infected with either shBmxA or negative control vectors. After 48 h, cells were counted and plated at 10,000 cells/well in duplicate within 96-well dishes. The cells were treated with either sham (0 Gy) or 2 Gy irradiation and incubated for 24h. Following this incubation, WST-1 labeling mixture was added to each well and analyzed at OD450 nm to determine mitochondrial viability. Normalized values for OD450 nm are shown as mean and standard error. Combined Bmx knockdown with irradiation decreases HUVEC survival.

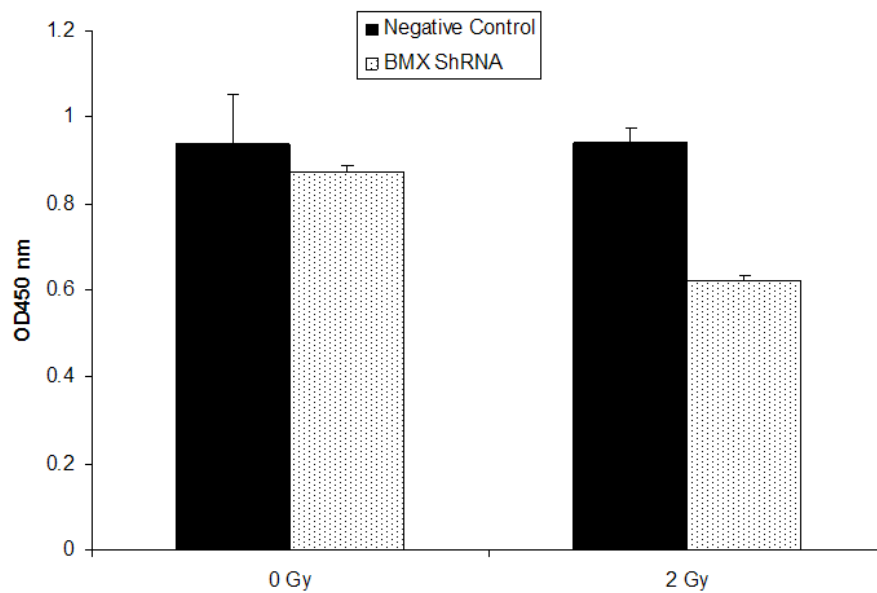
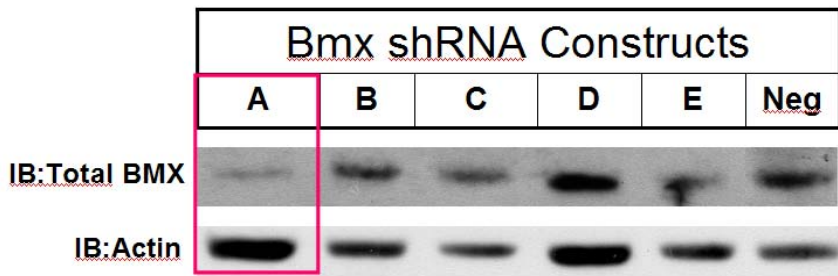


Figure 2. Retroviral shRNA knockdown of Bmx in HUVEC. A) shRNA retrovirus knockdown. Multiple shRNA retroviral plasmid constructs (Bmx constructs A-E, and negative control construct) were transfected into LiNX cells to produce retroviral supernatant. HUVEC were infected with the retroviral supernatants and incubated for 48 h. Cells were then harvested and total protein lysates were separated by SDS-PAGE. Western blot analysis using anti-Bmx antibody was used to detect total Bmx levels. B) MTT-based survival assay: cells infected with either Bmx or control shRNA were incubated for 48 h prior to plating of 10,000 cells/well in 96-well dishes. Cells were treated with either 0 or 2 Gy and incubated for 24 h. Cells were then treated with WST-1 reagent and incubated for 2h prior to dye quantification at OD 450 nm. Normalized mean absorbance values with standard errors are shown.

c) Construct stable prostate cancer cell lines that express inducible shRNA to Bmx and assay these cell lines for enhancement of radiation effect (Months 1-14).

We had significant difficulty in producing inducible shRNA vectors for Bmx. As detailed in part **b)** above, we have found an acceptable shRNA vector from a commercial source (Origene) for Bmx knockdown in HUVEC, but we have tried to generate similar constructs within an inducible retroviral vector, but we were not successful as of the completion of the grant in June 2008. We also tried to construct an inducible system, but we were unable to accomplish this. The non-inducible shRNA vectors shown in figure 2 that were successful in HUVEC do have mammalian antibiotic resistance for stable selection. Unfortunately, our attempts to make these stable Bmx knockdown clones in both DU145 and PC3 failed. It is possible that Bmx expression is vital for these prostate cancer cells to grow such that selection pressures prevented us from establishing effective knockdown in our experimentation.

d) Characterize the efficacy of Bmx specific inhibitors in enhancing radiation effect on endothelial cells and prostate cancer cells (Months 1-14).

As with the other sub-tasks for Task 1, our initial focus was to characterize HUVEC in terms of Bmx specific inhibitors. Due to the more extensive published data utilizing LFM-A13 in both *in vitro* and *in vivo* systems, we chose to study this drug in greater detail. The other inhibitors that have been considered include terreic acid and AG879. However, we did not have time to complete a full set of proposed experiments for those drugs. Moreover, the terreic acid appeared to be the most toxic of the three drugs.

Other consideration related to this task which was proposed as part of the future goals in the original proposal included the identification of novel Bmx inhibitors through Vanderbilt University Institute of Chemical Biology. Most importantly, a collaboration with the Department of Pharmacology was set up and is still ongoing to try to develop these Bmx inhibitors that may have better efficacy.

However, since the grant funding was stopped early due to my acceptance of a faculty position in July 2008, for this final report, the data presented below detail the use of the commercially available drug, LFM-A13 within HUVEC as well as some data for LFM-A13 in DU145 cells.

Pharmacological inhibition of Bmx

Having established that Bmx knockdown can enhance radiation efficacy in endothelial cells, we wanted to determine whether or not pharmacological inhibition of Bmx would show the same effect. Bmx specific inhibitors⁶⁻⁹ have been described, particularly LFM-A13, which targets the Tec family. Since Bmx is the only Tec family member expressed in endothelium, we studied this drug in HUVEC. The drug, LFM-A13 has been shown to block VEGF induced signaling through Bmx inhibition in HUVEC at a dose of 25 μ M. Therefore, we utilized 30 μ M LFM-A13 for *in vitro* studies. Figure 3A shows 3 μ M (subtherapeutic) vs. 30 μ M LFM-A13 pre-incubation on radiation-induced Bmx activation in the *in vitro* kinase assay at the time points with highest Bmx activation. As can be seen, 30 μ M but not 3 μ M LFM-A13 attenuates the activation of Bmx in response to 3 Gy.

Bmx inhibition attenuates endothelial cell viability

To determine whether LFM-A13 produces a radiosensitization effect in HUVEC, we studied clonogenic survival assays in HUVEC with LFM-A13 pre-incubation (Figure 3B). HUVEC were pre-treated with DMSO vehicle control or 30 μ M LFM-A13 45 min prior to irradiation with 0, 2, 4, or 6 Gy. Colonies were allowed to form over 10 days which were then counted and the surviving fraction was calculated for each radiation dose. These studies indicated that 30 μ M LFM-A13 can radiosensitize HUVEC compared to the control as evidenced by the statistically significant downward survival curve shift. The dose enhancing ratio (DER) was 1.47.

Apoptosis was studied to determine whether this is a mechanism of enhanced cytotoxicity. Figure 3C illustrates the effect of LFM-A13 on apoptosis within these cells. HUVEC treated with 30 μ M LFM-A13 or DMSO control were subjected to sham or 3 Gy irradiation and then incubated for 24 h prior to trypsinization and flow cytometric analysis. Annexin V-propidium iodide staining revealed that drug or 3 Gy alone was not capable of shifting cells into either early (Q4-1) or late (Q2-1) apoptosis but that the combination of LFM-A13 and 3 Gy caused a statistically significant ($p < 0.001$ vs. LFM-A13 or 3 Gy alone) increase in apoptosis. To confirm these findings, HUVEC were treated with either 30 μ M LFM-A13 or DMSO control with or without 3 or 6 Gy irradiation and incubated for 24 h. These cells were fixed and stained with DAPI and the percent of apoptotic cells was quantified. As shown in Figure 3D, the combination of LFM-A13 and irradiation resulted in enhancement of apoptosis (* indicates $p < 0.05$ vs. DMSO control and ** indicates $p < 0.001$ vs. LFM alone).

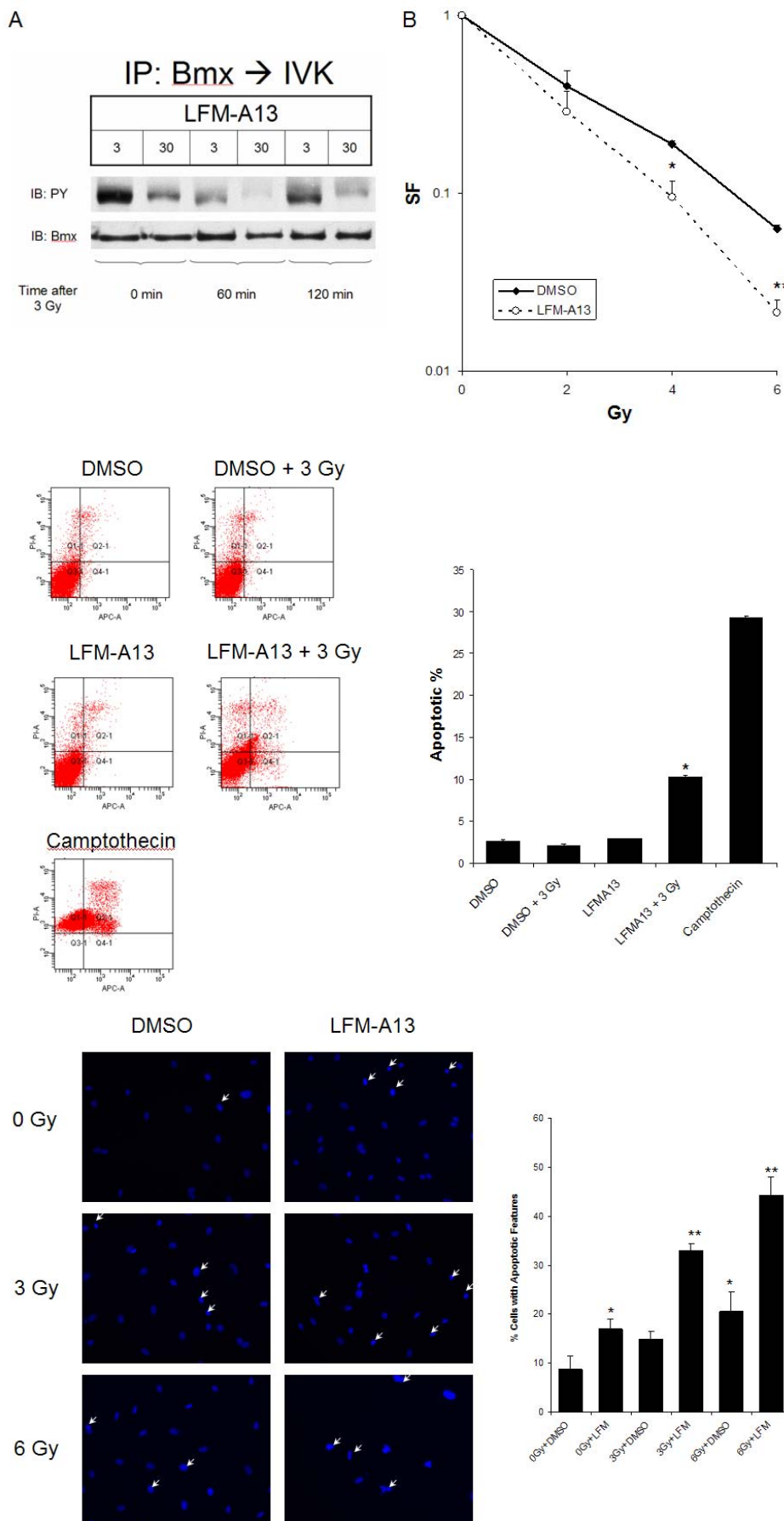


Figure 3. Radiation-induced endothelial cell cytotoxicity is enhanced by Bmx inhibition. A) *In vitro* kinase assay (IVK) for LFM-A13. Bmx was immunoprecipitated (IP:Bmx) from lysates of HUVEC pre-treated with either 3 or 30 μ M LFM-A13 for 60 min prior to 3 Gy irradiation and harvested at the indicated times. IP:Bmx samples were then eluted in non-denaturing conditions and subjected to kinase assay. Samples were then loaded for SDS-PAGE and anti-phosphotyrosine (IB:PY) Western blotting. Total Bmx levels were determined by anti-Bmx Western blotting (IB:Bmx). **B)** Clonogenic assay of HUVEC cells with 1 hour preincubation with 30 μ M LFM-A13 or DMSO vehicle control is shown. Cells were counted and plated and subjected to indicated doses of radiation and colonies formed over 10 days. Surviving colonies were plotted as a function of cells plated and normalized by the plating efficiency for each condition (Shown as surviving fraction, SF). SE Bars are shown. (*, $p=0.007$; **, $p=0.0002$) **C)** 30 μ M LFM-A13 vs. DMSO vehicle control was added to plated cells with or without 3 Gy radiation (IR) 60 min later. After 24h, cells were trypsinized and collected for flow cytometry using Annexin V/Propidium iodide staining. Percent cells undergoing early (Q4-1) and late (Q2-1) apoptosis were compared to viable cells (Q3-1) and dead cells (Q1-1) as indicated. Quantification of early + late apoptosis is shown graphically as mean and standard error. (*, $p<0.001$ vs. LFM-A13 or 3 Gy alone) **D)** Cells preincubated 60 min with 30 μ M LFM-A13 or DMSO vehicle control were treated with either 3 or 6 Gy of irradiation and incubated at 37° C for 24 h prior to fixing and staining with DAPI. Percent of cells demonstrating apoptotic morphology (marked by arrows) was calculated and is shown as mean and standard error. (*, $p<0.05$ vs. control; **, $p=0.001$ vs LFM-A13 alone).

Bmx inhibition attenuates endothelial cell function

Functional assays of endothelial cells include cell migration and capillary-like tubule formation. Figure 4A illustrates the effect of LFM-A13 and irradiation on endothelial migration across a gap (endothelial cell closure assay) at 12 and 24 h. HUVEC were plated on glass slides and grown to 80% confluency. A gap region, free of cells, was then created using a 200 μ l pipette tip. These slides were then treated with 30 μ M LFM-A13 or DMSO control for 45 min prior to either 0 or 3 Gy. Cells were fixed and stained at 12 or 24 h and photographs were taken of the gap region and the surrounding cells to determine the ability of the HUVEC to migrate across and fill the gap. Relative cell density was calculated for each condition to control for the cytotoxic effects of treatment as shown in Figure 4B. By 24 h, control cells effectively migrated across the gap. 30 μ M LFM-A13 or 3 Gy alone had minimal effect on attenuating endothelial cell closure at both 12 h and 24 h compared to vehicle treated control. However, the combination induced a greater than additive effect which was statistically significant (* indicates $p < 0.05$ vs. control, and ** is $p < 0.01$ vs. LFM-A13). Figure 4C and D show capillary tubule formation assay. HUVEC plated onto matrigel were treated with 30 μ M LFM-A13 or DMSO with or without 3 Gy irradiation and allowed to form tubules. The cells were then fixed and stained. The number of tubules were quantified and plotted. Representative photographs are shown in Figure 4C and quantified in Figure 4D. Cells that were treated with both LFM-A13 and 3 Gy showed a significant reduction ($p < 0.005$) in tubules formed compared to cells treated with either treatment alone.

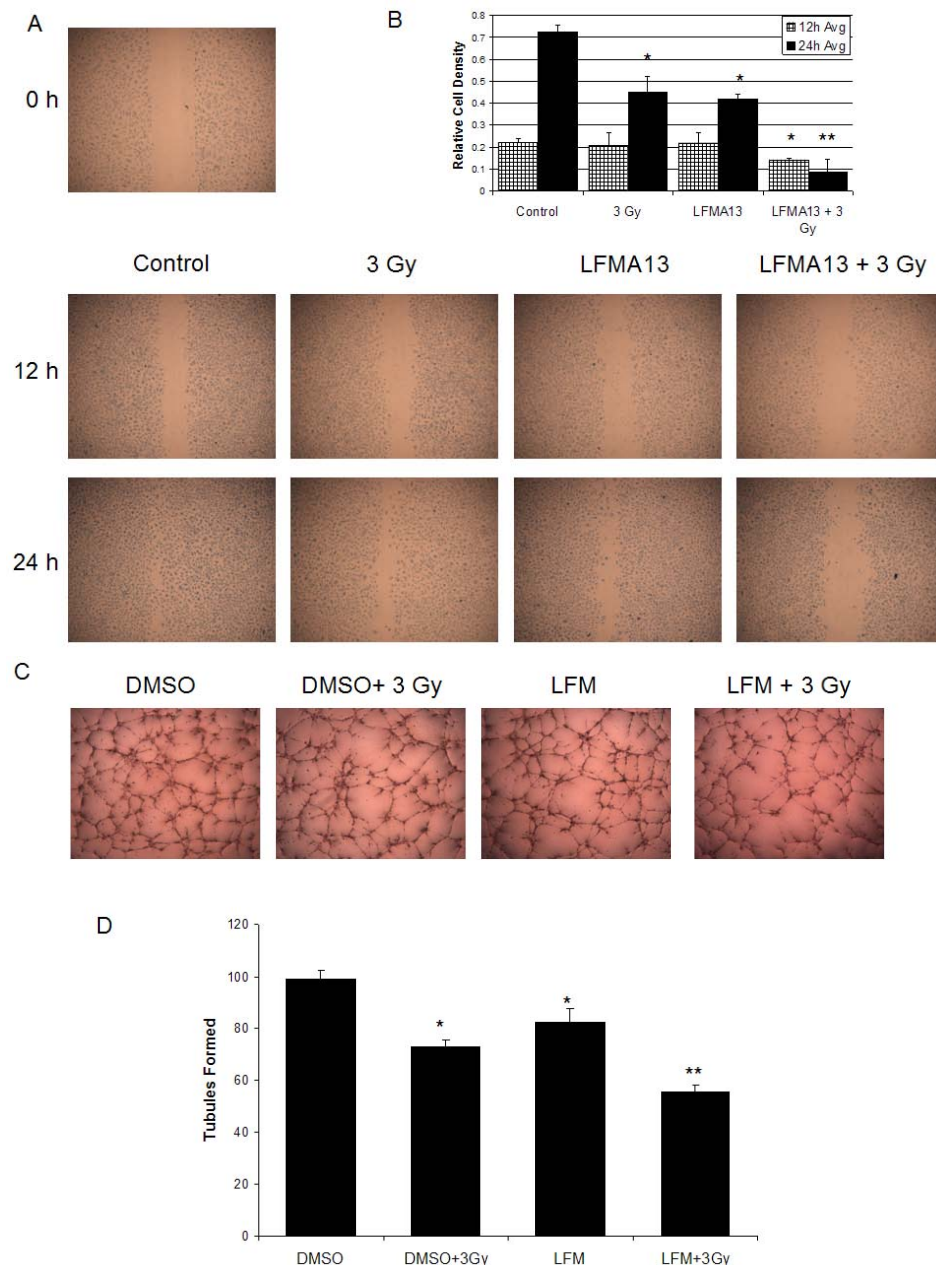


Figure 4. Endothelial cell function is attenuated by Bmx inhibition and radiation. A)

Endothelial cell closure assay is shown in which 80% confluent HUVEC were subjected to a gap formation using a 200 μ l pipette tip. Cells were then treated with 30 μ M LFM-A13 or DMSO vehicle control for one hour followed by 3 Gy. 12 and 24 h later, cells were fixed with 70% ethanol and stained with methylene blue. Shown are representative photographs. **B)** A bar graph of the mean and standard error of relative cell density in the original gap area ($n=4$) is shown. (*, $p < 0.05$ vs. control; **, $p < 0.01$ vs. LFM-A13 alone) **C)** HUVEC were placed onto Matrigel plugs and were treated with either 30 μ M LFM-A13 or DMSO vehicle control for 30 min followed by 3 Gy irradiation. The cells were then incubated and tubules were allowed to form as shown by the representative photographs. The cells were then fixed and tubules were quantitated by NIH ImageJ software. The mean number of tubules are shown in **D)** with standard error bars. (*, $p < 0.05$ vs. control; **, $p < 0.005$ vs. LFM-A13 or 3 Gy alone)

LFM-A13 produces modest radiosensitization in prostate cancer cells

To determine whether LFM-A13 produces a radiosensitization effect in prostate cancer cells, we studied clonogenic survival assays in DU145 cells with LFM-A13 pre-incubation (Figure 5). DU145 were pre-treated with DMSO vehicle control or 30 μ M LFM-A13 45 min prior to irradiation with 0, 2, 4, or 6 Gy. Colonies were allowed to form over 10 days which were then counted and the surviving fraction was calculated for each radiation dose. These studies indicated that 30 μ M LFM-A13 can radiosensitize DU145 compared to the control as evidenced by the statistically significant downward survival curve shift though this was more modest than what was seen in HUVEC.

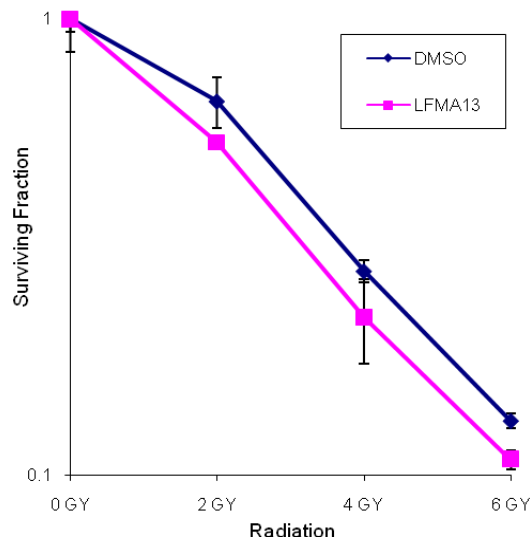


Figure 5. Radiation-induced prostate cancer cytotoxicity is modestly enhanced by Bmx inhibition. Clonogenic assay of DU145 human prostate cancer cells with 1 hour preincubation with 30 μ M LFM-A13 or DMSO vehicle control is shown. Cells were counted and plated and subjected to indicated doses of radiation and colonies formed over 10 days. Surviving colonies were plotted as a function of cells plated and normalized by the plating efficiency for each condition (Shown as surviving fraction, SF). SE Bars are shown.

Task 2. To determine the mechanism of radiation induced activation of Bmx (Months 3-18).

This task had the least amount of progress during the abbreviated award period. In terms of reagents to accomplish the sub-tasks for Task 2, we did have both adenoviruses for c-Src and PI3K and specific drugs, however, for Task 2b, we were unable to construct the domain mutants for Bmx prior to June 2008 when I left Vanderbilt University to accept my faculty position at The University of Alabama at Birmingham. We had pursued collaborative help to produce these mutants in hopes of getting the assays done before the award period was finished, but we were unable to do so. We still intend to construct these mutants, but based on the negative tumor growth delay data as shown in Figure 7 and described in Task 3, we decided to limit our efforts towards the mutant construction at this time. However, once we are able to obtain the mutants, they can be transfected into the prostate cancer cell lines, DU145, LNCaP and PC3, but in order to have efficient expression in HUVEC, we will still need to place those mutants within an adenovirus or lentiviral vector system. Viral infection is required for HUVEC as we have tried several different transfection methods, including electroporation (Amaxa system) and New England Biolabs HUVEC TransPass reagent, which have only resulted in significant toxicity to the cells and very little transfection efficiency. Therefore, this task will require significantly more time to be accomplished due to the time and expense of creating viruses. As such, the descriptions below detail the proposed studies for these sub-tasks.

a) Treat endothelial cells and prostate cancer cell lines with specific inhibitors (drugs and adenoviruses) to c-Src and PI3K and analyze for attenuation of radiation-induced Bmx activation (Months 3-18).

Several experiments will be undertaken. First, we will treat HUVEC with pharmacological inhibitors of c-Src (SU6656) and PI3K (IC486068) prior to irradiation and then probe for Bmx activation using the Bmx immunoprecipitation with *in vitro* kinase assay as shown in Figure 1. We and others have previously published data using specific inhibitors for these kinases.¹⁰⁻¹⁵ A second set of experiments planned for this sub-task involves the use of dominant negative c-Src, dominant negative PI3K, and control GFP adenoviruses that we

already possess in our lab. We will express these adenoviruses in HUVEC and probe for Bmx activation in response to radiation. The last set of experiments will focus on the various prostate cancer cell lines (DU145, LNCaP and PC3).

b) Construct a series of Bmx functional domain mutants, express them in endothelial cells and prostate cancer cell lines, and analyze for attenuation of radiation-induced Bmx activation (Months 3-18).

We will transfect into prostate cancer cell lines and infect into HUVEC, Bmx and Bmx mutants with immunoaffinity tags (hemagglutinin) that we generate from our expression plasmid vector system to determine which functional domain(s) are critical for radiation induced activation. Several groups have used this technique to characterize Bmx interaction with other proteins.¹⁶⁻²⁰ The following point mutations will be generated using site directed mutagenesis: 1) Kinase dead – K444Q^{16, 18}; 2) Dominant negative – K444Q, E42K¹⁶; 3) Constitutive membrane association – E42K¹⁹; 4) PH domain mutant – R29C¹⁹; 5) SH2 domain mutant – R322V¹⁷; 6) SH3 domain mutants – Y215F²¹. We plan to use immunoprecipitation of the immunoaffinity tag with subsequent *in vitro* kinase assay similar to what is shown in Figure 1 in order to determine activity.

Task 3. To determine whether specific inhibitors of Bmx enhance the therapeutic efficacy of radiotherapy in prostate cancer tumor models (Months 9-24).

For this task, we were able to perform some intriguing experiments looking at therapeutic potential within an *in vivo* model system. Because we were able to demonstrate that Bmx inhibition sensitizes the vascular endothelial cells to ionizing radiation as shown in the Task 1 report, we initiated studies looking at the effect of Bmx inhibition within prostate cancer xenografts in athymic nude mice. The initial Doppler sonography (Figure 6) was encouraging since the antivasculature effect seemed to be confirmed *in vivo*. Unfortunately, this did not translate into enhanced radiation efficacy in terms of tumor growth delay (Figure 7) although each treatment group was superior to control. Due to the abbreviated award period, once again, we were unable to complete all subtasks so only the description of the proposed Task 3b is detailed.

a) Perform *in vivo* testing of tumor response to Bmx inhibitors and radiation in human prostate cancer xenografts in athymic nude mice (Months 9-24).

Bmx inhibition attenuates tumor blood flow

To test the effects of Bmx inhibition *in vivo*, LFM-A13 was used to treat mice harboring DU145 prostate tumor xenografts. Power-weighted pixel density measurements using Doppler sonography showed that ionizing radiation combined with LFMA13 resulted in a dramatic decrease in tumor blood flow compared to DMSO vehicle control or either treatment alone as shown in Figure 6.

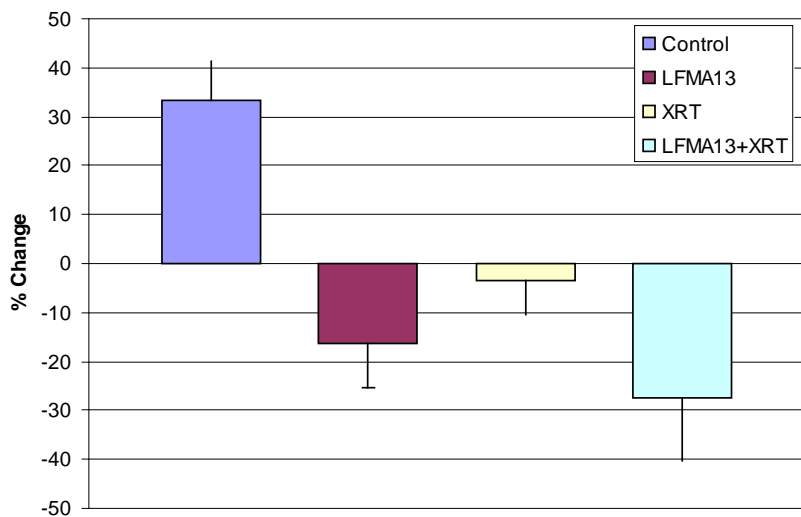


Figure 6. Tumor blood flow is reduced by Bmx inhibition and radiation. DU145 prostate cells were injected into the hind limb of athymic nude mice and were allowed to form tumor xenografts. Once the tumors were detectable, 30 μ M LFMA13 or DMSO vehicle control was injected into the peritoneum (I.P.) for five consecutive days with or without 2.5 Gy radiation (XRT) delivered 30 minutes after each injection for a total of 12.5 Gy. Power-weighted pixel density measurements of tumor blood flow were assessed using doppler ultrasound on day 1 and day 5. The % change in mean density measurement and standard errors are shown.

Combination of Bmx inhibition and irradiation did not yield enhanced treatment effect in terms of tumor growth delay

We implanted DU145 cells into the hind limbs of athymic nude mice and tested the Bmx/Etk inhibitors, LFM-A13, ability to control tumor growth. As shown in Figure 7, the animals were randomized to four treatment groups: 1) Control group – received vehicle control daily for five days; 2) Drug alone – received drug alone for five days; 3) radiation alone – daily 3 Gy radiation for five days; 4) Drug plus radiation – received drug 30 min to 1 h prior to daily 3 Gy radiation treatment for five days. Tumor volumes were measured every two days using a skin caliper to measure (a) length, (b) width, (c) depth. Tumor volume was then calculated from the formula $(a \times b \times c)/2$ derived from the ellipsoid formula. Unfortunately, we saw a paradoxical effect of combination treatment relative to what was shown in the *in vitro* model systems and the power-weighted pixel density measurements. Nevertheless, each treatment group was superior to control suggesting that drug scheduling relative to irradiation needs to be optimized to confirm that combination treatment is not more effective than either treatment alone. However, based on time constraints, we were unable to do this during the award period.

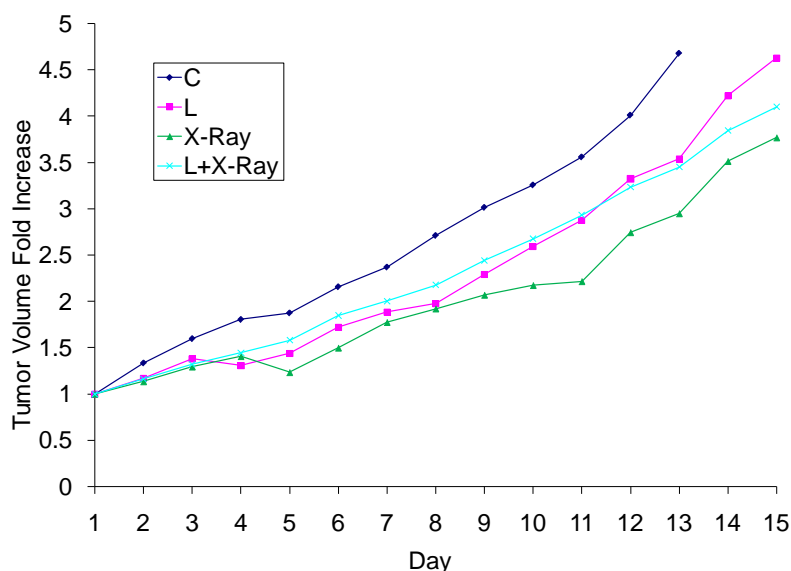


Figure 7. Tumor growth delay does not occur with combination treatment. DU145 prostate cells were injected into the hind limb of athymic nude mice and were allowed to form tumor xenografts. Once the tumors were detectable, 30 μ M LFMA13 (L) or DMSO vehicle control (C) was injected into the peritoneum (I.P.) for five consecutive days with or without 2.5 Gy radiation (X-Ray) delivered 30 minutes after each injection for a total of 12.5 Gy. Mean tumor volume was measured using a skin caliper to measure (a) length, (b) width, (c) depth. Tumor volume was calculated from the formula $(a \times b \times c)/2$ derived from the ellipsoid formula and mean tumor volume fold increase was plotted over time for each treatment group.

b) Perform *in vivo* testing of tumor response to Bmx inhibitors and radiation in transgenic mice that spontaneously form prostate cancers within the prostate (Months 9-24).

The prostate epithelial specific long probasin promoter and the SV40 large T antigen (LPB12T-7) transgenic mice express an androgen-dependent promoter (LPB) that causes animals to spontaneously form large vascular tumors within the prostate. These mice form extensive high grade prostate intraepithelial neoplastic (HGPIN) lesions as well as invasive lesions with neuroendocrine differentiation.^{22, 23} Because these tumors retain androgen sensitivity, we can also determine the effect of androgen deprivation on Bmx activity and radiation sensitivity. This has clinical significance as patients with intermediate and high risk factors receive androgen ablation during radiation therapy.

Proposed Studies

We will treat these animals with radiation and Bmx inhibitors and analyze for tumor response at the end of a specified period of time. We will analyze the differential effect of treatment on the vascular component of the tumor as well as within the tumor itself. We will perform immunohistochemical staining of the tumor endothelium and analyze frozen tissue samples with immunoprecipitation and Western blot analysis for Bmx as described above. We will perform this in both castrated and noncastrated mice to determine if there is an interaction between androgen receptor signaling and the radiation and Bmx inhibition.

KEY RESEARCH ACCOMPLISHMENTS

- Bmx is activated by clinically relevant doses of ionizing radiation in vascular endothelial cells
- Bmx inhibition with shRNA retroviral knockdown enhances radiation cytotoxicity within vascular endothelial cells
- Bmx inhibition with LFM-A13 when combined with radiation attenuates vascular endothelial cell function and enhances radiation cytotoxicity in vascular endothelial cells and prostate cancer cells.
- Ionizing radiation combined with Bmx inhibition using LFM-A13 attenuates tumor blood flow in mouse model of prostate cancer
- Bmx inhibition results in tumor growth delay in mouse model of prostate cancer.
- Combination of Bmx inhibition with ionizing radiation, paradoxically, did not enhance prostate tumor growth control based on hind limb tumor growth delay of prostate cancer.

REPORTABLE OUTCOMES

Willey CD, Tu T, Thotala D, Geng L, Hallahan DE. The identification of Bmx as a molecular target for radiosensitization of lung cancer. Oral and poster presentation, AACR Advances and Challenges in Aerodigestive Epithelial Cancer conference, Charleston, SC, February 2007

NCI Joint Lung and Head/Neck SPORE Travel Award – Charleston, SC, February 2007

Tu T, Thotala D, Hallahan DE, **Willey CD**. Bmx is a vascular endothelial molecular target for radiosensitization. Poster Discussion. ASTRO Convention, Los Angeles, CA, October 2007.

Hallahan D.E. and **Willey C.D.** (2007). "BMX as a Molecular Target for Radiosensitizing Agents." (*Patent application submitted; Ser. No. 60/997,124*)

Tu T, Thotala D, Geng L, Hallahan DE, **Willey CD**. Bmx is activated by ionizing radiation and is a molecular target for development for Radiosensitizing drugs. Cancer Research. 2008 Apr 15;68(8):2861-9.

Lastly, this work has helped me to attain a faculty position as a physician scientist in radiation oncology. I accepted a position as assistant professor at the University of Alabama at Birmingham in the Department of Radiation Oncology and started on July 1, 2008. Because of this change from postdoctoral fellow to a junior faculty member, I was unable to complete the remainder of the grant proposal.

CONCLUSION

We have determined that the non-receptor tyrosine kinase, Bmx, is activated by ionizing radiation within vascular endothelium. In addition, the preliminary studies from the training grant proposal as well as review of the literature identify Bmx as highly expressed within prostate cancer and prostate cancer cell lines. Therefore, understanding the role of Bmx within prostate cancer and its vasculature may provide a new strategy for prostate cancer treatment.

Our studies, thus far, have shown that Bmx inhibition, with both pharmacologic agents and molecular manipulation, can enhance the therapeutic effect of ionizing radiation on vascular endothelial cells and prostate cancer cells. Furthermore, examination of prostate cancer xenografts within mice confirm these findings as combined Bmx inhibition with radiation results in significant drop in tumor blood flow. Interestingly, Bmx inhibition did lead to tumor growth delay for in vivo prostate cancer xenografts but, paradoxically, no radiation enhancement was seen when drug was combined with radiation.

In summary, Bmx is a new molecular target for radiation sensitization based on *in vitro* and *in vivo* experimentation in vascular endothelium. Ongoing Bmx inhibitor drug development may allow for improved systemic control of prostate cancer. However, how best to combine Bmx inhibition with irradiation remains unclear. Ultimately, clinical evaluation of Bmx inhibitors with radiation will be critical during the development of Bmx as a biological target for therapy.

REFERENCES

1. Pollack, A., *et al.* (2002) Prostate cancer radiation dose response: results of the M. D. Anderson phase III randomized trial. *Int J Radiat Oncol Biol Phys* 53, 1097-1105
2. Chung, L.W., *et al.* (2005) Molecular insights into prostate cancer progression: the missing link of tumor microenvironment. *J Urol* 173, 10-20
3. Padhani, A.R., *et al.* (2005) Angiogenesis imaging in the management of prostate cancer. *Nat Clin Pract Urol* 2, 596-607
4. Charlesworth, P.J., and Harris, A.L. (2006) Mechanisms of disease: angiogenesis in urologic malignancies. *Nat Clin Pract Urol* 3, 157-169
5. Chen, R., *et al.* (2001) Regulation of the PH-domain-containing tyrosine kinase Etk by focal adhesion kinase through the FERM domain. *Nat Cell Biol* 3, 439-444
6. He, H., *et al.* (2004) The Tyr-kinase inhibitor AG879, that blocks the ETK-PAK1 interaction, suppresses the RAS-induced PAK1 activation and malignant transformation. *Cancer Biol Ther* 3, 96-101
7. Uckun, F.M., *et al.* (2002) In vivo pharmacokinetic features, toxicity profile, and chemosensitizing activity of alpha-cyano-beta-hydroxy-beta-methyl-N-(2,5-dibromophenyl)propenamide (LFM-A13), a novel antileukemic agent targeting Bruton's tyrosine kinase. *Clin Cancer Res* 8, 1224-1233
8. Mahajan, S., *et al.* (1999) Rational design and synthesis of a novel anti-leukemic agent targeting Bruton's tyrosine kinase (BTK), LFM-A13 [alpha-cyano-beta-hydroxy-beta-methyl-N-(2, 5-dibromophenyl)propenamide]. *J Biol Chem* 274, 9587-9599
9. Kawakami, Y., *et al.* (1999) Terreic acid, a quinone epoxide inhibitor of Bruton's tyrosine kinase. *Proc Natl Acad Sci U S A* 96, 2227-2232
10. Cuneo, K.C., *et al.* (2006) SRC family kinase inhibitor SU6656 enhances antiangiogenic effect of irradiation. *Int J Radiat Oncol Biol Phys* 64, 1197-1203
11. Contessa, J.N., *et al.* (2005) Compensatory ErbB3/c-Src signaling enhances carcinoma cell survival to ionizing radiation. *Breast Cancer Res Treat*, 1-11
12. Geng, L., *et al.* (2004) A specific antagonist of the p110delta catalytic component of phosphatidylinositol 3'-kinase, IC486068, enhances radiation-induced tumor vascular destruction. *Cancer Res* 64, 4893-4899
13. Edwards, E., *et al.* (2002) Phosphatidylinositol 3-kinase/Akt signaling in the response of vascular endothelium to ionizing radiation. *Cancer Res* 62, 4671-4677
14. Lu, B., *et al.* (2005) The use of tyrosine kinase inhibitors in modifying the response of tumor microvasculature to radiotherapy. *Technol Cancer Res Treat* 4, 691-698
15. Tan, J., and Hallahan, D.E. (2003) Growth factor-independent activation of protein kinase B contributes to the inherent resistance of vascular endothelium to radiation-induced apoptotic response. *Cancer Res* 63, 7663-7667
16. Pan, S., *et al.* (2002) Etk/Bmx as a tumor necrosis factor receptor type 2-specific kinase: role in endothelial cell migration and angiogenesis. *Mol Cell Biol* 22, 7512-7523
17. Abassi, Y.A., *et al.* (2003) p130Cas Couples the tyrosine kinase Bmx/Etk with regulation of the actin cytoskeleton and cell migration. *J Biol Chem* 278, 35636-35643
18. Tsai, Y.T., *et al.* (2000) Etk, a Btk family tyrosine kinase, mediates cellular transformation by linking Src to STAT3 activation. *Mol Cell Biol* 20, 2043-2054.
19. Ekman, N., *et al.* (2000) The Bmx tyrosine kinase is activated by IL-3 and G-CSF in a PI-3K dependent manner. *Oncogene* 19, 4151-4158
20. Kim, O., *et al.* (2002) Selective activation of small GTPase RhoA by tyrosine kinase Etk through its pleckstrin homology domain. *J Biol Chem* 277, 30066-30071
21. Nore, B.F., *et al.* (2003) Identification of phosphorylation sites within the SH3 domains of Tec family tyrosine kinases. *Biochim Biophys Acta* 1645, 123-132
22. Kasper, S., *et al.* (1998) Development, progression, and androgen-dependence of prostate tumors in probasin-large T antigen transgenic mice: a model for prostate cancer. *Lab Invest* 78, i-xv
23. Kasper, S. (2005) Survey of genetically engineered mouse models for prostate cancer: analyzing the molecular basis of prostate cancer development, progression, and metastasis. *J Cell Biochem* 94, 279-297

APPENDICES

Tu T, Thotala D, Geng L, Hallahan DE, **Willey CD**. Bmx is activated by ionizing radiation and is a molecular target for development for Radiosensitizing drugs. *Cancer Research*. 2008 Apr 15;68(8):2861-9.

Bone Marrow X Kinase–Mediated Signal Transduction in Irradiated Vascular Endothelium

Tianxiang Tu,¹ Dinesh Thotala,¹ Ling Geng,¹ Dennis E. Hallahan,^{1,2,3} and Christopher D. Willey¹

Departments of ¹Radiation Oncology and ²Cancer Biology, and ³Vanderbilt-Ingram Cancer Center, Vanderbilt University School of Medicine, Nashville, Tennessee

Abstract

Radiation-induced activation of the phosphatidyl inositol-3 kinase/Akt signal transduction pathway requires Akt binding to phosphatidyl-inositol phosphates (PIP) on the cell membrane. The tyrosine kinase bone marrow X kinase (Bmx) binds to membrane-associated PIPs in a manner similar to Akt. Because Bmx is involved in cell growth and survival pathways, it could contribute to the radiation response within the vascular endothelium. We therefore studied Bmx signaling within the vascular endothelium. Bmx was activated rapidly in response to clinically relevant doses of ionizing radiation. Bmx inhibition enhanced the efficacy of radiotherapy in endothelial cells as well as tumor vascular endothelium in lung cancer tumors in mice. Retroviral shRNA knockdown of Bmx protein enhanced human umbilical vascular endothelial cell (HUVEC) radiosensitization. Furthermore, pretreatment of HUVEC with a pharmacologic inhibitor of Bmx, LFM-A13, produced significant radiosensitization of endothelial cells as measured by clonogenic survival analysis and apoptosis as well as functional assays including cell migration and tubule formation. *In vivo*, LFM-A13, when combined with radiation, resulted in significant tumor microvascular destruction as well as enhanced tumor growth delay. Bmx therefore represents a molecular target for the development of novel radiosensitizing agents. [Cancer Res 2008;68(8):2861–9]

Introduction

The microvasculature is a major component of cancer and supports tumor growth. We and others have studied the inherent resistance of tumor vascular endothelium to cytotoxic effects of ionizing radiation. Ionizing radiation activates signal transduction through the phosphatidyl inositol-3 kinase (PI3K)/Akt pathway, which enhances endothelial cell viability (1–3). Akt activity is critical for this process because dominant-negative Akt mutant (Thr308Ala and Ser473Ala) overexpression in endothelial cells abrogates radiation-induced cell survival response (4). Moreover, we have previously shown that ionizing radiation–induced Akt activation is eliminated by overexpression of mutant p85 component of PI3K (5). Mutant p85 functions as a dominant negative by preventing activation of p110 catalytic subunit of PI3K. This inhibition prevents the production of phosphatidylinositol phosphates (PIP) that activate Akt, resulting in enhanced radiation effect. Therefore, inhibition of the PI3K signal transduction pathway can abrogate the endothelial cell survival signaling mediated by Akt.

Although the PI3K/Akt pathway is a major contributor to radiation resistance seen in tumor microvasculature, other pathways activated shortly after ionizing radiation are also being investigated. Indeed, the activation of Akt has been shown to be critically dependent on binding of the pleckstrin homology domain of Akt to specific PIPs, phosphatidylinositol(3,4,5)-triphosphate, in particular, which allows the colocalization of Akt with upstream activators (6). Bone marrow X kinase (Bmx), also known as epithelial and endothelial tyrosine kinase, contains a pleckstrin homology domain as well as Src homology (SH)2 and SH3 domains capable of interacting with several types of second messengers and adaptor proteins that are present in human umbilical vein endothelial cells (HUVEC; refs. 7–13). Bmx is the ubiquitously expressed member of the Tec family of nonreceptor tyrosine kinases with high expression in lung, prostate, and the heart (10, 11). In addition, salivary epithelium, granulomonocytic cells, endothelial cells, and epithelial cells express this protein in relatively high amounts (10, 11, 14–16). Bmx seems to act both upstream and downstream of PI3K (7, 10, 11, 17–21). Bmx also interacts with G-proteins (10, 22–24), integrins/NRTKs (7, 25), tumor necrosis factor receptors (9), as well as various protein tyrosine phosphatases (26) and lipid phosphatases (27).

Because Bmx seems to potentiate proliferative and cell survival signaling in many cell types, we investigated Bmx signaling transduction during the radiation response in vascular endothelium. In the present study, radiation-induced Bmx activation in vascular endothelium was investigated. We show that inhibition of Bmx activity enhances the effectiveness of radiation on vasculature. These findings support the hypothesis that Bmx promotes a cell survival pathway and is a molecular target for drug development in the treatment of cancer.

Materials and Methods

Cell culture. HUVECs were purchased from Clonetics and maintained in EBM-2 medium supplemented with EBM-2 singlequots (Cambrex). HUVECs were limited to passages 3 to 6. Lewis Lung carcinoma (LLC) cells were purchased from American Type Tissue Culture and maintained in DMEM supplemented with 10% fetal bovine serum (FBS) and 1% penicillin-streptomycin. Cell lines were incubated at 37°C in a 5% CO₂ incubator.

LFM-A13 (30 μmol/L *in vitro* or 50 mg/kg, *i.p.* *in vivo*) and DMSO were obtained from Sigma. Drug was administered to cells 30 to 60 min before irradiation. A Mark-1 Irradiator ¹³⁷Cs (JL Shepard and Assoc.) was used to irradiate HUVEC cultures at a dose rate of 1.897 Gy/min.

Retrovirus production and HUVEC infection. Negative control and Bmx shRNA retroviral constructs were purchased from OriGene, Inc. A total of five different constructs (labeled Bmx A–E) were tested for Bmx knockdown in HUVEC. The retroviruses were produced according to manufacturer's protocol with some modifications. LINX packaging cell line, purchased from Open Biosystems, was grown on 10-cm tissue culture plates to 30% to 40% confluency in medium containing DMEM with 10% FBS [complete growth medium (CGM)] with hygromycin, penicillin, and streptomycin supplementation. These cells were then transfected with

Requests for reprints: Christopher D. Willey, Department of Radiation Oncology, 1301 22nd Avenue South, B-902 The Vanderbilt Clinic, Nashville, TN 37232-5671. Phone: 615-322-2555; Fax: 615-343-6589; E-mail: christopher.willey@vanderbilt.edu.
©2008 American Association for Cancer Research.
doi:10.1158/0008-5472.CAN-07-5743

retroviral plasmid DNA by incubation with 5 mL transfection mix for 4 to 6 h. The transfection mix contained 12 µg of shRNA retroviral vector DNA within 600 µL serum-free DMEM without antibiotics, and 240 µL of room temperature Arrest-In transfection reagent (Open Biosystems) within 4.4 mL serum-free DMEM without antibiotics, which was prepared and kept at room temperature for 45 min before transfection to allow for transfection complexes to be formed. After initial 4- to 6-h transfection, 5 mL of CGM were added and incubated overnight. The medium was changed and the cells were incubated for at least an additional 24 h. Supernatant was collected and filtered through a 45-µm filter to produce the viral stock.

For HUVEC infection, HUVECs were grown on tissue culture plates to 50% confluency. On the day of infection, the HUVECs were incubated in medium containing 5 µg/mL polybrene for 4 h before infection. Medium was then removed and 1.5 mL of virus supernatant supplemented with 5 µg/mL polybrene were added directly to the cells and allowed to adsorb for 40 to 60 min, and then 7 mL of HUVEC medium containing 5 µg/mL of polybrene were added, and the cells were incubated for 24 h. The medium was changed to regular HUVEC growth medium, and the cells were incubated for an additional 2 d to allow for Bmx knockdown.

Cell lysis and immunoblot analysis. HUVECs of passage 3 to 6 were treated with or without Bmx inhibition (LFM-A13 for 60 min or shRNA retrovirus infection 48 h before) followed by irradiation and then harvested at the indicated times. Cells were processed and immunoblotted as described previously (28). Antibodies were as follows: PY20HRP (BD Biosciences), actin (Sigma-Aldrich), Bmx and PY40 Bmx (Cell Signaling Technology), phospho-Akt (S473), Akt (Cell Signaling Technology), as well as horseradish peroxidase-labeled mouse anti-rabbit secondary antibodies (Sigma-Aldrich) except for PY20HRP, which was prelabeled. Films were scanned into Adobe Photoshop with subsequent densitometry analysis using NIH Image J 1.37v. Experiments were performed at least thrice.

Immunoprecipitation and *in vitro* kinase assay. HUVECs of passage 3 to 6 were grown to 70% to 80% confluency and then serum starved for 5 h. The cells were then treated with sham or 3 Gy irradiation. After treatment, the cells were incubated at 37°C with 5% CO₂ for the indicated times. For inhibition studies, inhibitor was added at a 1:1,000 dilution 60 min before irradiation. After incubation, the tissue culture dishes were placed on ice and washed twice with ice cold 1× PBS followed by lysis using 400 µL M-PER containing protease and phosphatase inhibitors (Sigma) for 5 min. The cells were scraped and transferred to Eppendorf tubes, vortexed for 20 sec, and incubated on ice for 30 min. After clearing the lysate by centrifugation at 15,000 *g* for 15 min at 4°C, the supernatant was quantified for protein concentration using bicinchoninic acid method before immunoprecipitation. Immunoprecipitation was performed using the Catch and Release v 2.0 system (Upstate) according to manufacturer's protocol with some modification. Briefly, spin columns containing binding resin were prepared by washing twice with 1× wash buffer (2,000 *g*/30 sec). After column preparation, 500 µg of cell lysate were combined with 2 µg of anti-Bmx antibody (H-220; Santa Cruz Biotechnology, Inc.), 10 µL of affinity ligand, and enough 1× wash buffer to have a 500 µL final volume. This was added to the capped spin column that was rotated end-over-end overnight at 4°C. The spin column was washed thrice with 1× wash buffer followed by elution using 70 µL of 1× nondenaturing elution (native protein elution) buffer. For *in vitro* kinase assay, 35 µL of eluate were then combined with 25 µL of kinase buffer containing 25 mmol/L Tris (pH 7.5), 5 mmol/L β-Glycerophosphate, 2 mmol/L DTT, 0.1 mmol/L Na₂VO₄, and 10 mmol/L MgCl₂ with 1 µL of 10 mmol/L ATP, and this was incubated for 20 min at 37°C. The reaction was stopped by adding 20 µL of 4× SDS sample buffer and boiled for 5 min. Samples were then run on SDS-PAGE and anti-PY20HRP (BD Biosciences) and anti-Bmx (Cell Signaling Technology). Western blotting was performed to identify phosphorylated protein bands at 75 to 80 kDa. Densitometric analysis was performed using NIH Image J.

WST-1 assay. This assay is a modification of an 3-(4,5-dimethylthiazol-2-yl)-2,5-diphenyltetrazolium bromide (MTT) assay and was performed per manufacturer's protocol (Calbiochem). Briefly, HUVEC were infected with shRNA retrovirus, and after 48 h of incubation, cells were lifted by trypsinization, were counted, and were plated at 10,000 cells per well of 96-well microtiter plates in duplicate. These plates were then subjected to 0

or 2 Gy and incubated for 24 h at 37°C with 5% CO₂. After incubation, 10 µL of WST-1 labeling mixture was added to each well and mixed gently before returning to the incubator for 2 h. Absorbance at 450 nm was measured on a microplate reader and results were plotted using Microsoft Excel Software.

Clonogenic survival. LLC or passage 3 to 6 HUVECs were grown to 70% to 80% confluency. Cells were washed with 1× PBS, trypsin suspended, and were counted and adjusted to specific densities for each condition. The cells were then plated on tissue culture plates and allowed to attach for 4 h. LFM-A13 or DMSO was added at a 1:1,000; dilution followed 60 min later by 0, 2, 4, or 6 Gy. Medium was changed after irradiation. Ten to fourteen days after irradiation, the plates were fixed with 70% ethanol and stained with 1% methylene blue. Colonies were then counted using a dissection microscope with positive colonies containing at least 50 cells. Surviving fraction was calculated by the equation (number of colonies formed/number of cells plated)/(number of colonies for sham irradiated group/number of cells plated). Dose-enhancing ratios were calculated by dividing the dose (Gy) for radiation alone by the dose for radiation plus treatment (normalized for plating efficiency of treatment) for which a surviving fraction of 0.2 is achieved. These results were then plotted in a semilogarithmic format using Microsoft Excel software.

Endothelial cell tubule formation assay. HUVEC of passage 3 to 6 were grown to 70% to 80% confluency. Cells were then washed with 1× PBS and suspended by trypsinization. Cells were counted and adjusted to 2.5 to 5 × 10⁴ cells per mL in medium. Seventy-five microliters of Matrigel (BD Biosciences) were plated into each well of a 96-well plate and allowed to polymerize at 37°C. Cell suspensions (200 µL; 8–12 × 10³ cells) were added to each well. After 30 min, DMSO control or LFM-A13 was added. Thirty minutes later, dishes were treated with sham or 3 Gy and were then incubated until tubules had formed in control plates (4–6 h). Digital photographs were taken of individual wells and tubules were counted by an observer blinded to the treatment conditions. The mean and SE were calculated (*n* = 3).

Endothelial closure assay. HUVEC of passage 3 to 6 were grown on glass slides and were subjected to gap formation as described previously (28). Cells were treated with LFM-A13 or DMSO control before 0 or 3 Gy and incubated for the indicated times. Photographs of cell defect and surrounding cells were taken, and relative cell density within the defect was calculated as follows: (number of cells/original cell defect area)/(number of cells/surrounding area).

Apoptosis assays. HUVEC were grown to 70% to 80% confluency before treatment with LFM-A13 or DMSO control. Cells were then irradiated with 0 or 3 Gy and harvested 24 h after irradiation. Annexin V-FITC Apoptosis Detection kit (BD PharMingen) was used to stain cells [propidium iodide (50 ng) and Annexin V-FITC (5 ng) were added to 10⁵ cells] for flow cytometry according to manufacturer's protocol. For each treatment, the percentage of cells undergoing apoptosis (±SE) was calculated. Camptothecin (5 µmol/L) treatment for 6 h served as positive control.

HUVEC were also assayed for apoptosis using a 4',6-diamidino-2-phenylindole (DAPI) staining of the nuclei to identify cells undergoing morphologic changes. Seventy to eighty percent confluent HUVECs were treated with or without LFM-A13, incubated for 1 h, and then irradiated at 3 Gy. Cells were returned to the incubator for an additional 24 h before DAPI staining. Multiple high powered fields (at least seven) were examined by an observer who was blinded to the experimental conditions for each of the cultures. The percentage of cells demonstrating apoptotic nuclei were quantified. The mean and SE were calculated for each treatment group.

Tumor vascular window model. We have previously described the tumor vascular window model technique (29). Briefly, three mice for each group had LLC tumors grown within a vascular window such that tumor vasculature could be visualized within window frames containing a coordinate system for serial photography. Animals were treated with LFM-A13 by i.p. injection 60 min before 2 Gy irradiation using an 80 kVp superficial X-ray machine (Pantak X-ray Generator). Serial color photographs were taken to document blood vessel appearance on days 0 to 7. Photographs were scanned and processed using Adobe Photoshop software (Adobe) to mark the center of vessels, verified by an observer blinded to treatment groups. Vascular length density (VLD) was quantified for each microscopic field using ImagePro Plus v. 5.1 software (Media Cybernetics,

Inc.). The mean and SE of VLD in each treatment group were calculated and plotted. All animals used were cared for according to Vanderbilt University's Institutional Animal Care and Use Committees guidelines.

Tumor immunohistochemistry. LLCs were s.c. injected into the hind limb of C57/BL6 mice to form syngeneic homografts. When tumors grew to 200 mm³, (~7 d) the mice were treated with five consecutive daily treatments of i.p. LFM-A13 followed 45 min later by 3 Gy irradiation using an 80-kVp superficial X-ray generator. Twelve hours after the last radiation treatment, mice were sacrificed and tumors were harvested, fixed in paraffin, and sectioned by the Vanderbilt University Immunohistochemistry Core Facility as we have described previously (28). Immunostaining was with goat anti-CD34 (Santa Cruz Biotechnology), and microvascular photos were analyzed using ImagePro software with pixel number quantified.

Tumor growth delay. LLCs were s.c. injected into the hind limb of C57/BL6 mice to form syngeneic homografts. When tumors grew to 200 mm³, (~7 d) the mice were treated with five consecutive daily treatments of i.p. LFM-A13 followed 45 min later by 3 Gy irradiation using an 80 kVp superficial X-ray generator. Serial measurements of tumor dimensions were taken by caliper, and tumor volume was calculated using the modified ellipsoid formula (length × width × depth)/2. The mean and SE were plotted using Microsoft Excel software.

Statistical analysis. The mean and SEs for all assays were calculated using Microsoft Excel software. Student's *t* test was performed to determine *P* values between treatment groups. *P* values of ≤0.05 were considered statistically significant.

Results

Bmx is activated in endothelium upon irradiation. We examined primary culture vascular endothelial cells (HUVEC) to determine whether Bmx was activated by ionizing radiation, because of its similarities in structure and signaling with that of Akt, and was possibly contributing to radiation resistance. Figure 1A shows a time course of Bmx activation upon irradiation with a clinically relevant dose of 2 Gy. Tyr⁴⁰, present in the pleckstrin homology domain of Bmx, becomes phosphorylated during its activation (7). Bmx is phosphorylated at 60 minutes after 2 Gy of irradiation. To confirm this finding, we used an *in vitro* kinase assay in which Bmx was immunoprecipitated from irradiated or sham-irradiated endothelial cells and then incubated with ATP in a kinase reaction. These samples were then run on SDS-PAGE and probed for antiphosphotyrosine to analyze autophosphorylation of Bmx. As shown in Fig. 1B, Bmx was activated after irradiation. Examination of total Bmx revealed no change in Bmx levels at any of the time points that were assayed. Densitometric quantitation (mean and SE) from four separate experiments is shown as well. Interestingly, Bmx showed significant kinase activity immediately after irradiation and then has a second peak of lesser activity at 1 hour.

Bmx knockdown enhances radiation efficacy in endothelium.

Because we were able to detect a clear activation of Bmx after a clinically relevant dose of ionizing radiation, we wanted to determine whether Bmx activation protects the endothelial cells from cytotoxic damage. Because primary culture endothelial cells, such as HUVEC, have low transfection yields, we used a retroviral shRNA system to knockdown Bmx levels before irradiation. Figure 2A shows five different retroviral constructs (A through E) for Bmx as well as a negative control construct (*Neg*) that were used to infect HUVEC. After 48 hours, infected cells were harvested and lysates were prepared for total Bmx Western blotting. As can be seen, construct A (shBmxA) provided ~90% knockdown of Bmx protein levels compared with the negative control shRNA vector. Bmx knockdown experiments were performed with or without irradiation. Figure 2B shows MTT-based (WST-1) survival assay with HUVEC infected with either shBmxA or negative control vectors. After 48 hours, cells were counted and plated at 10,000 cells per well in duplicate within 96-well dishes. The cells were treated with either sham (0 Gy) or 2 Gy irradiation and incubated for 24 hours. After this incubation, WST-1 labeling mixture was added to each well and analyzed at absorbance at 450 nm to determine mitochondrial viability. Normalized values for absorbance at 450 nm are shown as mean and SE. Combined Bmx knockdown with irradiation decreases HUVEC survival.

Pharmacologic inhibition of Bmx. Having established that Bmx knockdown can enhance radiation efficacy in endothelial cells, we wanted to determine whether or not pharmacologic inhibition of Bmx would show the same effect. Bmx-specific inhibitors (30–33) have been described, particularly LFM-A13, which targets the Tec family. Because Bmx is the only Tec family member expressed in endothelium, we studied this drug in HUVEC. The drug, LFM-A13, has been shown to block vascular endothelial growth factor (VEGF)-induced signaling through Bmx inhibition in HUVEC at a dose of 25 μmol/L. Therefore, we used 30 μmol/L LFM-A13 for *in vitro* studies. Figure 3A shows 3 μmol/L (subtherapeutic) versus 30 μmol/L LFM-A13 preincubation on radiation-induced Bmx activation in the *in vitro* kinase assay at

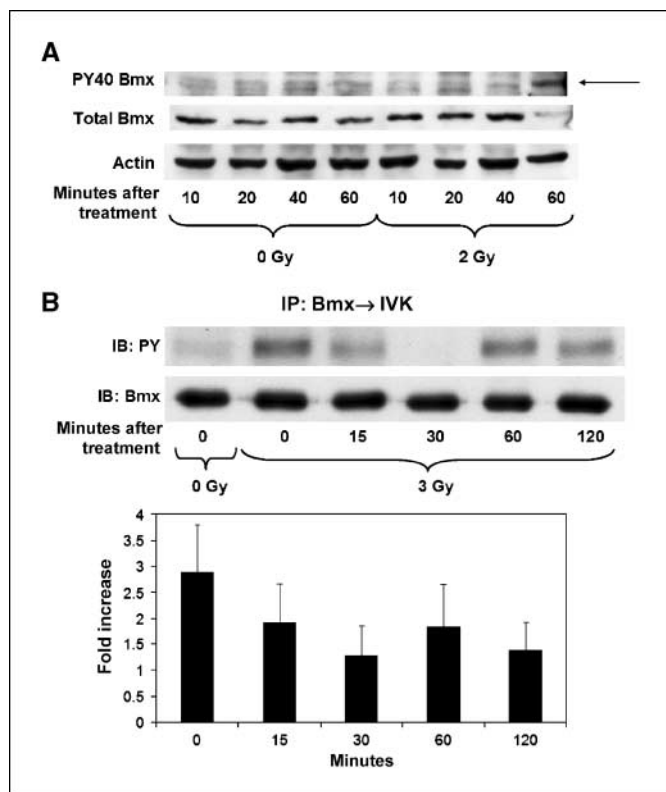


Figure 1. Bmx is activated by radiation in endothelial cells. HUVEC were either sham irradiated or irradiated with 2 Gy. *A*, cells were harvested and total lysates were made after incubation at 37°C for the indicated times in minutes. Western blots are shown of phosphotyrosine 40 (PY40) Bmx, indicative of activation, as well as total Bmx and actin for normalization. *B*, *in vitro* kinase (IVK). Bmx was immunoprecipitated (IP:Bmx) from the lysates and eluted under nonreducing conditions. After elution, kinase assay buffer was added for 20 min. Samples were separated by SDS-PAGE. Western blot analysis using antiphosphotyrosine (IB:PY) antibody was used to detect autophosphorylation. Total Bmx levels are also shown (IB:Bmx) using anti-Bmx antibody. Densitometric quantitation of autophosphorylation was performed (*n* = 4); columns, mean fold increase over 0 Gy conditions; bars, SE.

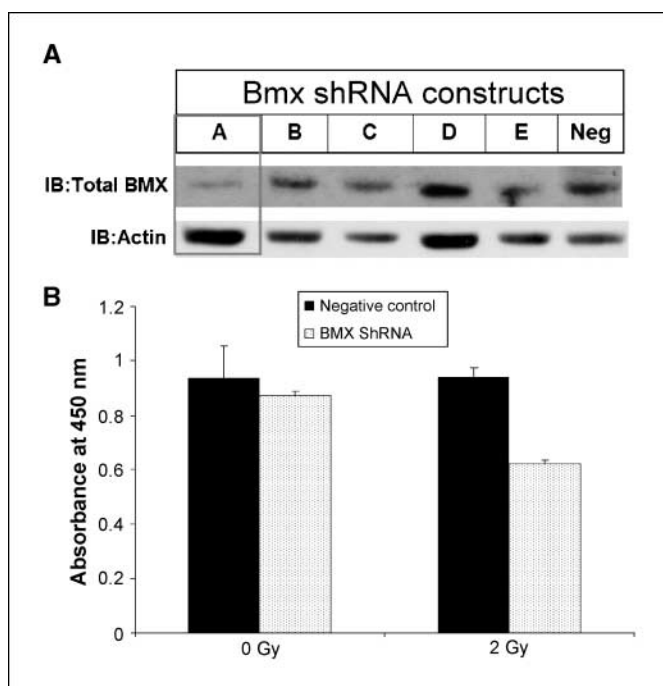


Figure 2. Retroviral shRNA knockdown of Bmx in HUVEC. **A**, shRNA retrovirus knockdown. Multiple shRNA retroviral plasmid constructs (Bmx constructs A–E and negative control construct) were transfected into LiNX cells to produce retroviral supernatants as described in Materials and Methods. HUVEC were infected with the retroviral supernatants and incubated for 48 h. Cells were then harvested and total protein lysates were separated by SDS-PAGE. Western blot analysis using anti-Bmx antibody was used to detect total Bmx levels. **B**, MTT-based survival assay; cells infected with either Bmx or control shRNA were incubated for 48 h before plating of 10,000 cells per well in 96-well dishes. Cells were treated with either 0 or 2 Gy and incubated for 24 h. Cells were then treated with WST-1 reagent and incubated for 2 h before dye quantification at absorbance at 450 nm. Columns, normalized mean absorbance values; bars, SE.

the time points with highest Bmx activation. As can be seen, 30 $\mu\text{mol/L}$ but not 3 $\mu\text{mol/L}$ LFM-A13 attenuates the activation of Bmx in response to 3 Gy.

Bmx inhibition attenuates endothelial cell viability. To determine whether LFM-A13 produces a radiosensitization effect in HUVEC, we studied clonogenic survival assays in HUVEC with LFM-A13 preincubation (Fig. 3B). HUVEC were pretreated with DMSO vehicle control or 30 $\mu\text{mol/L}$ LFM-A13 45 minutes before irradiation with 0, 2, 4, or 6 Gy. Colonies were allowed to form >10 days, which were then counted, and the surviving fraction was calculated for each radiation dose. These studies indicated that 30 $\mu\text{mol/L}$ LFM-A13 can radiosensitize HUVEC compared with the control as evidenced by the statistically significant downward survival curve shift. The dose enhancing ratio was 1.47.

Apoptosis was studied to determine whether this is a mechanism of enhanced cytotoxicity. Figure 3C illustrates the effect of LFM-A13 on apoptosis within these cells. HUVEC treated with 30 $\mu\text{mol/L}$ LFM-A13 or DMSO control were subjected to sham or 3 Gy irradiation and then incubated for 24 hours before trypsinization and flow cytometric analysis. Annexin V–propidium iodide staining revealed that drug or 3 Gy alone was not capable of shifting cells into either early (Q4-1) or late (Q2-1) apoptosis but that the combination of LFM-A13 and 3 Gy caused a statistically significant ($P < 0.001$ versus LFM-A13 or 3 Gy alone) increase in apoptosis. To confirm these findings, HUVEC were treated with either 30 $\mu\text{mol/L}$ LFM-A13 or DMSO control with or without 3 or

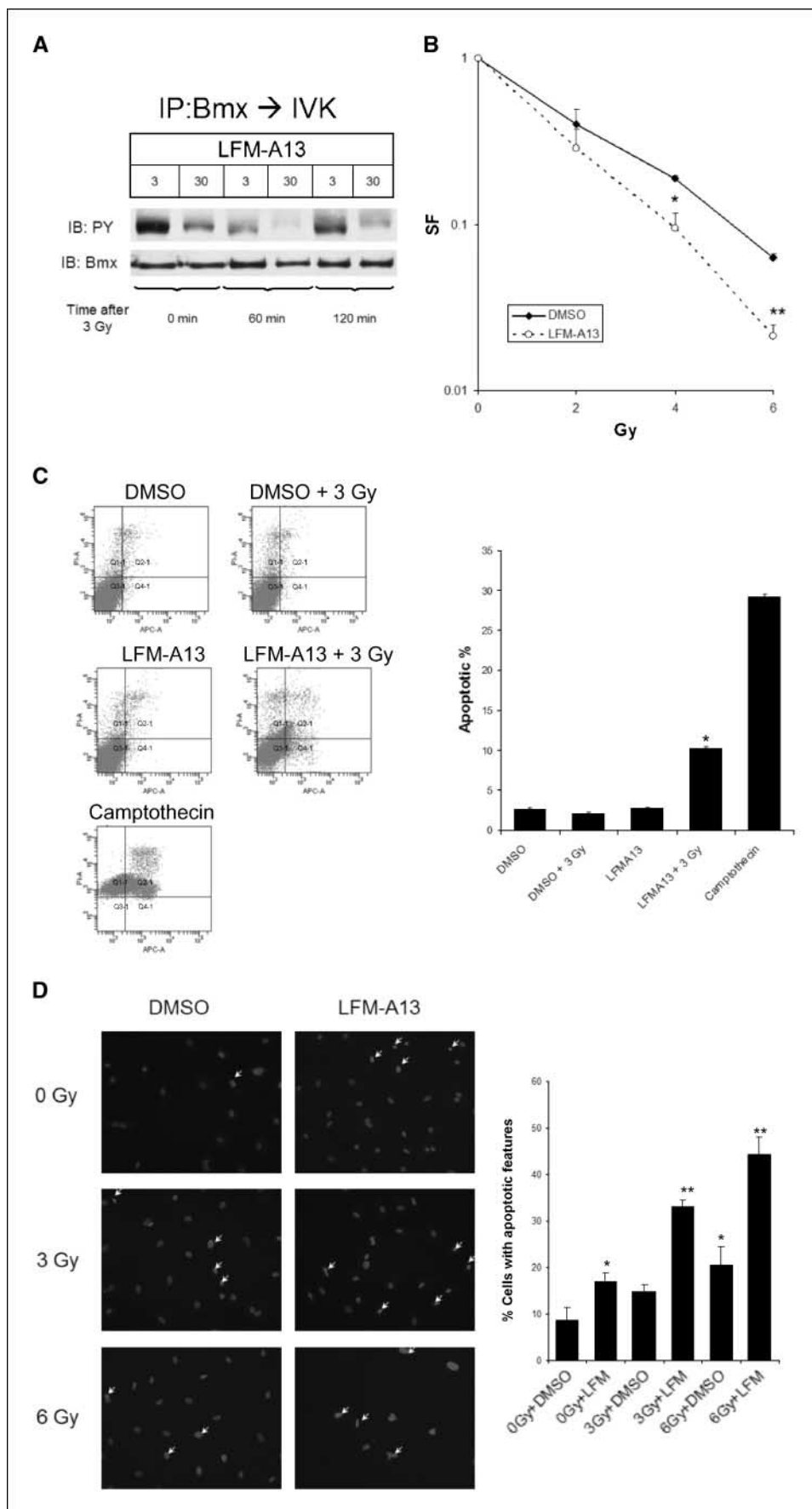
6 Gy irradiation and incubated for 24 hours. These cells were fixed and stained with DAPI, and the percentage of apoptotic cells was quantified. As shown in Fig. 3D, the combination of LFM-A13 and irradiation resulted in enhancement of apoptosis (*, $P < 0.05$ versus DMSO control; **, $P < 0.001$ versus LFM alone).

Bmx inhibition attenuates endothelial cell function. Functional assays of endothelial cells include cell migration and capillary-like tubule formation. Figure 4A illustrates the effect of LFM-A13 and irradiation on endothelial migration across a gap (endothelial cell closure assay) at 12 and 24 hours. HUVEC were plated on glass slides and grown to 80% confluency. A gap region, free of cells, was then created using a 200- μL pipette tip. These slides were then treated with 30 $\mu\text{mol/L}$ LFM-A13 or DMSO control for 45 minutes before either 0 or 3 Gy. Cells were fixed and stained at 12 or 24 hours, and photographs were taken of the gap region and the surrounding cells to determine the ability of the HUVEC to migrate across and fill the gap. Relative cell density was calculated for each condition to control for the cytotoxic effects of treatment as shown in Fig. 4B. By 24 hours, control cells effectively migrated across the gap. Thirty micromoles of LFM-A13 or 3 Gy alone had minimal effect on attenuating endothelial cell closure at both 12 and 24 hours compared with vehicle-treated control. However, the combination induced a greater than additive effect that was statistically significant (*, $P < 0.05$ versus control; **, $P < 0.01$ versus LFM-A13). Figure 4C and D show capillary tubule formation assay. HUVEC plated onto Matrigel were treated with 30 $\mu\text{mol/L}$ LFM-A13 or DMSO with or without 3 Gy irradiation and allowed to form tubules. The cells were then fixed and stained. The number of tubules were quantified and plotted. Representative photographs are shown in Fig. 4C and quantified in Fig. 4D. Cells that were treated with both LFM-A13 and 3 Gy showed a significant reduction ($P < 0.005$) in tubules formed compared with cells treated with either treatment alone.

Bmx inhibition attenuates tumor vasculature. To determine whether Bmx inhibition enhances radiation-induced destruction of tumor vasculature *in vivo*, we used i.p. injection of LFM-A13 before irradiation. A tumor vascular window chamber was placed on the dorsum of the C57BL6 mice, and LLC cells were implanted within the dorsal skin fold to allow for visualization of intravital tumor vasculature. Serial photographs were taken of the same region of the tumor, allowing for assessment of blood vessel formation and destruction. Figure 5A shows the effect of a single 50 mg/kg i.p. administration of LFM-A13 before 2 Gy irradiation. Representative photographs show that combination treatment results in dramatic reduction in tumor blood vessels. These results were quantified for each treatment condition as mean VLD with SE (Fig. 5B; $P < 0.0014$ versus LFM-A13 or 2 Gy alone). To confirm these findings, we used a hind limb syngeneic homograft model for determining vascular density within tumor sections. LLCs were implanted into the hind limbs of C57BL6 mice, and after tumors were formed, they were subjected to either daily LFM-A13 (50 mg/kg i.p. injection) or DMSO, followed 45 minutes later by 3 Gy or sham irradiation for a total of five treatments. The tumors were then harvested and prepared for immunohistochemistry analysis. Vessels were stained by anti-CD34 as shown in Fig. 5C, and these were quantified as shown in Fig. 5D. As can be seen, combination treatment was most effective at attenuating blood vessel formation ($P = 0.043$ versus ionizing radiation; $P = 0.0001$ versus LFM-A13 or vehicle control).

Bmx inhibition did not affect radiation sensitivity of LLC. Although we have shown the enhancement of radiation by Bmx inhibition within vascular endothelium, we determined whether

Figure 3. Radiation-induced endothelial cell cytotoxicity is enhanced by Bmx inhibition. **A**, *in vitro* kinase for LFM-A13. Bmx was immunoprecipitated from lysates of HUVEC pretreated with either 3 or 30 $\mu\text{mol/L}$ LFM-A13 for 60 min before 3 Gy irradiation and harvested at the indicated times. Immunoprecipitated Bmx samples were then eluted in nondenaturing conditions and subjected to kinase assay. Samples were then loaded for SDS-PAGE and antiphosphotyrosine Western blotting. Total Bmx levels were determined by anti-Bmx Western blotting. **B**, clonogenic assay of HUVEC cells with 1 h preincubation with 30 $\mu\text{mol/L}$ LFM-A13 or DMSO vehicle control is shown. Cells were counted and plated and subjected to indicated doses of radiation and colonies formed over 10 d. Surviving colonies were plotted as a function of cells plated and normalized by the plating efficiency for each condition (SF, surviving fraction). Points, mean; bars, SE. *, $P = 0.007$; **, $P = 0.0002$. **C**, 30 $\mu\text{mol/L}$ LFM-A13 versus DMSO vehicle control was added to plated cells with or without 3 Gy radiation (ionizing radiation) 60 min later. After 24 h, cells were trypsinized and collected for flow cytometry using Annexin V–propidium iodide staining. Percentage of cells undergoing early (Q4-1) and late (Q2-1) apoptosis were compared with viable cells (Q3-1) and dead cells (Q1-1) as indicated. Quantification of early + late apoptosis is shown graphically as mean and SE. *, $P < 0.001$ versus LFM-A13 or 3 Gy alone. **D**, cells preincubated 60 min with 30 $\mu\text{mol/L}$ LFM-A13 or DMSO vehicle control were treated with either 3 or 6 Gy of irradiation and incubated at 37°C for 24 h before fixing and staining with DAPI. Percentage of cells demonstrating apoptotic morphology (arrows) was calculated and is shown as mean and SE. *, $P < 0.05$ versus control; **, $P = 0.001$ versus LFM-A13 alone.



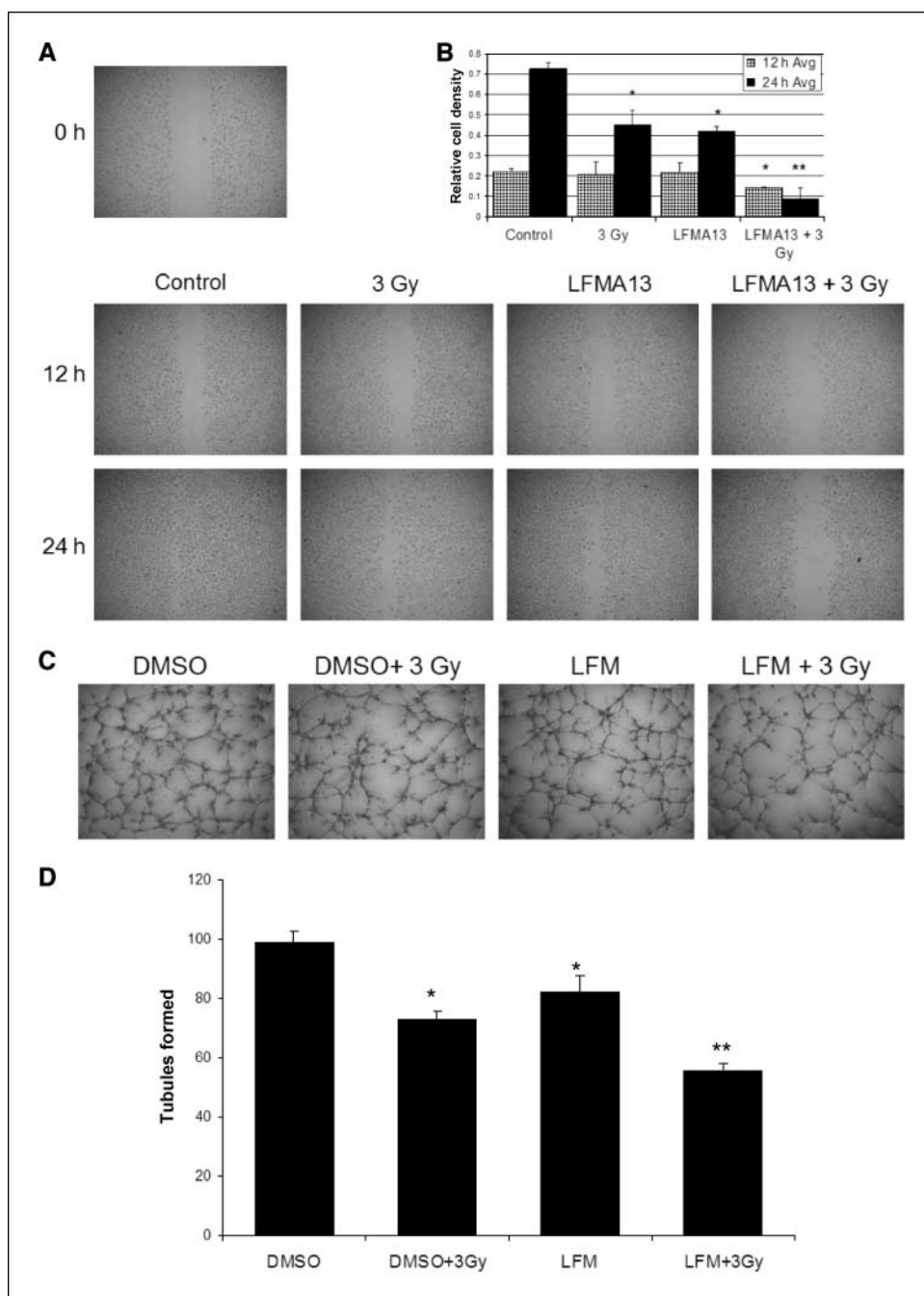


Figure 4. Endothelial cell function is attenuated by Bmx inhibition and radiation. **A**, endothelial cell closure assay is shown in which 80% confluent HUVEC were subjected to a gap formation using a 200 μ L pipette tip. Cells were then treated with 30 μ M/L LFM-A13 or DMSO vehicle control for 1 h followed by 3 Gy. Twelve and twenty-four hours later, cells were fixed with 70% ethanol and stained with methylene blue. Shown are representative photographs. **B**, relative cell density in the original gap area. Columns, mean ($n = 4$); bars, SE. *, $P < 0.05$ versus control; **, $P < 0.01$ versus LFM-A13 alone. **C**, HUVEC were placed onto Matrigel plugs and were treated with either 30 μ M/L LFM-A13 or DMSO vehicle control for 30 min followed by 3 Gy irradiation. The cells were then incubated, and tubules were allowed to form as shown by the representative photographs. The cells were then fixed, and tubules were quantitated by NIH ImageJ software. Columns, mean number of tubules; bars, SE. *, $P < 0.05$ versus control; **, $P < 0.005$ versus LFM-A13 or 3 Gy alone.

Bmx inhibition could also affect radiation sensitization in the lung cancer cell line (LLC). As shown in Fig. 6A, LFM-A13 showed no difference in clonogenic survival compared with DMSO control in LLCs. This suggests that LFM-A13 enhancement of radiation was limited to its antivasculature effect in this tumor model.

Bmx inhibition enhances radiation efficacy in tumor growth delay. Although LFM-A13 did not affect the radiosensitivity of the LLCs, LFM-A13 could still enhance radiation effects *in vivo* as an antivasculature treatment. To determine whether treatment with LFM-A13 could enhance tumor growth delay in irradiated tumors, mice bearing LLC hind limb tumors were treated, as in Fig. 5C, with i.p. injection of 50 mg/kg LFM-A13 or DMSO 45 minutes before 3 Gy or sham irradiation for 5 consecutive days. The mean tumor

volume and SE are plotted for each treatment group in Fig. 6B. Whereas LFM-A13 or radiation treatment alone resulted in a small growth delay, combination treatment showed a statistically significant enhancement of growth delay ($P = 0.027$). The fold increase in tumor volume at day 13 is also shown as mean and SE. These data suggest that LFM-A13 can enhance the efficacy of therapeutic radiation.

Discussion

The purpose of this study was to determine the role of Bmx in the radiation response of tumor vasculature. We and others have shown that radiation induces Akt phosphorylation (4, 29, 34–36).

Because the pleckstrin homology domains of Bmx and Akt bind the same phosphatidyl-inositol (3, 4, 5) phosphate, we hypothesized that Bmx might have a similar activation profile in response to ionizing radiation. Activation of Bmx occurred at clinically relevant doses of radiation: 2 to 3 Gy. Interestingly, we did note two waves of activation in the *in vitro* kinase assay. The early and more pronounced activation occurred immediately after irradiation, whereas the later wave occurred after 30 minutes and was less pronounced. It is possible that the second wave represents a "maturation event" such as phosphorylation of Tyr⁴⁰ within the pleckstrin homology domain. Phosphorylation of this site has been shown to correlate with FAK activation in other cell types (7). shRNA knockdown of Bmx resulted in radiation sensitization in HUVEC, suggesting that Bmx inhibition may be a promising pharmacologic target for radiation enhancement. Although LFM-A13 is clinically used as a Btk inhibitor, many groups have used LFM-A13 as a Bmx inhibitor due to the high homology between

Bmx and Btk. Because Btk is only found in bone marrow-derived cells, we felt that LFM-A13 could be used effectively for Bmx inhibition in our model systems. As we show in the *in vitro* kinase assay, LFM-A13 effectively attenuates Bmx activation in response to radiation. To confirm that this drug was not blocking all pleckstrin homology domain-containing kinases, we performed a time course and dose response of LFM-A13 with irradiation. Even at doses as high as 100 μ mol/L, we saw no attenuation of radiation-induced Akt phosphorylation indicative of its activation (data not shown). This drug that specifically targets Bmx not only enhanced the cytotoxic effects of irradiation on HUVEC but also inhibited the function of these cultured endothelial cells. Apoptosis and clonogenic studies revealed that LFM-A13 was capable of inducing radiosensitization in HUVEC. Moreover, LFM-A13 in combination with radiation resulted in dramatic effects on endothelial cell migration as evidenced by the endothelial closure assay and tubule formation assay.

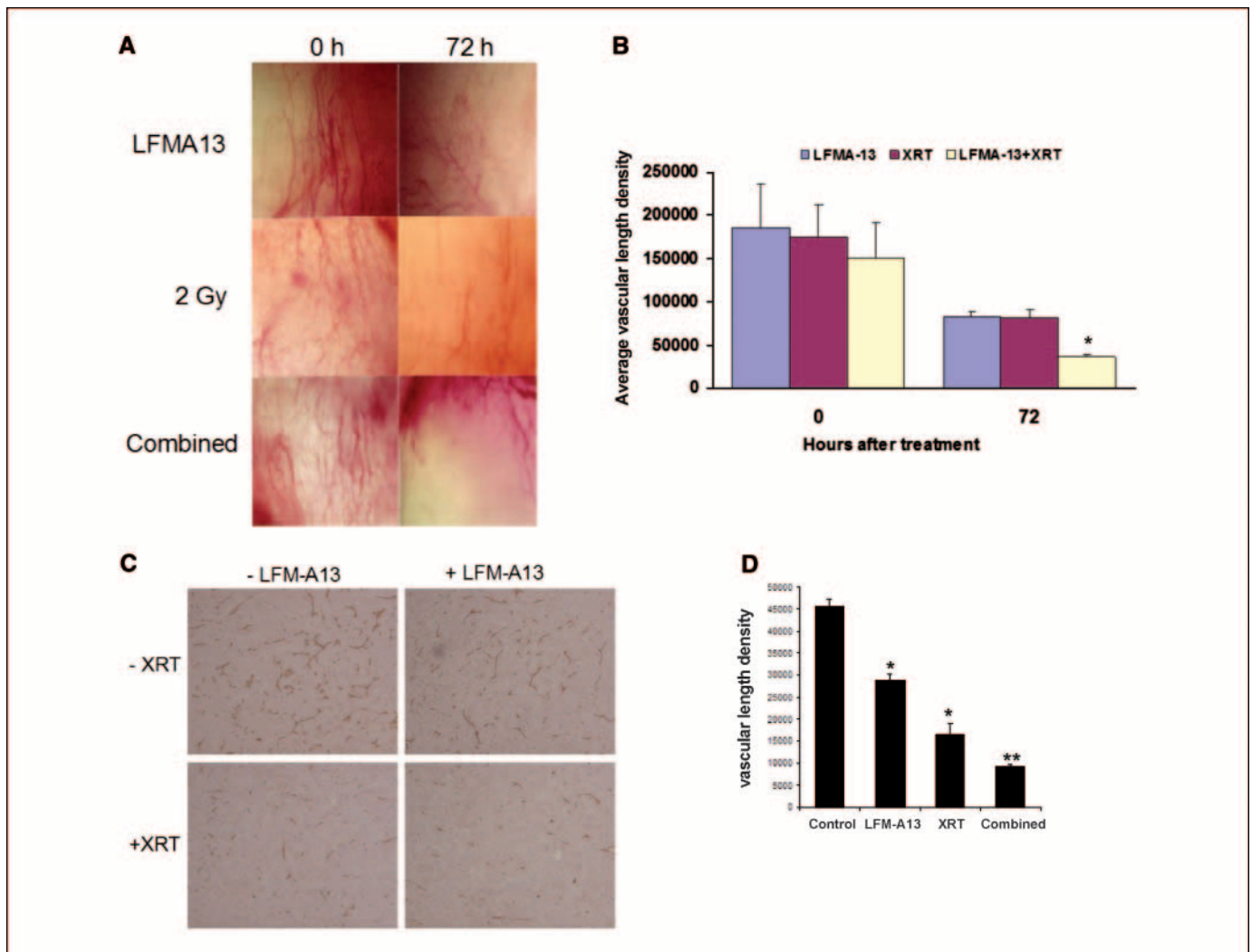


Figure 5. Tumor vascular destruction is enhanced by Bmx inhibition and radiation. Tumor vascular window model: A transparent window chamber was placed onto the dorsal skin fold of C57BL/6 mice to allow for visualization of blood vessels. LLC cells were injected into the chamber, and once vessels formed (6–8 d), the mice were treated with one i.p. dose of 50 mg/kg LFM-A13 or DMSO vehicle control for 1 h followed by 0 or 2 Gy. Microscopic photos were taken daily and the density of blood vessels was quantified for each treatment group. **A**, representative photographs. **B**, columns, mean VLD for each treatment group ($n = 3$); bars, SE. *, $P < 0.0014$ versus LFM-A13 or 3 Gy alone. **C**, LLC cells were implanted into the hind limb of mice. Once tumors formed, the mice were treated with five consecutive daily treatments of 50 mg/kg LFM-A13 (+LFM-A13) or DMSO control (–LFM-A13) and/or 3 Gy fractions (XRT). Tumors were harvested and stained for anti-CD34. Microscopic photos of immunohistochemistry. **D**, columns, mean level of CD34 staining for each treatment condition; bars, SE. **, $P = 0.043$ versus ionizing radiation; *, $P = 0.0001$ versus LFM-A13 or vehicle control.

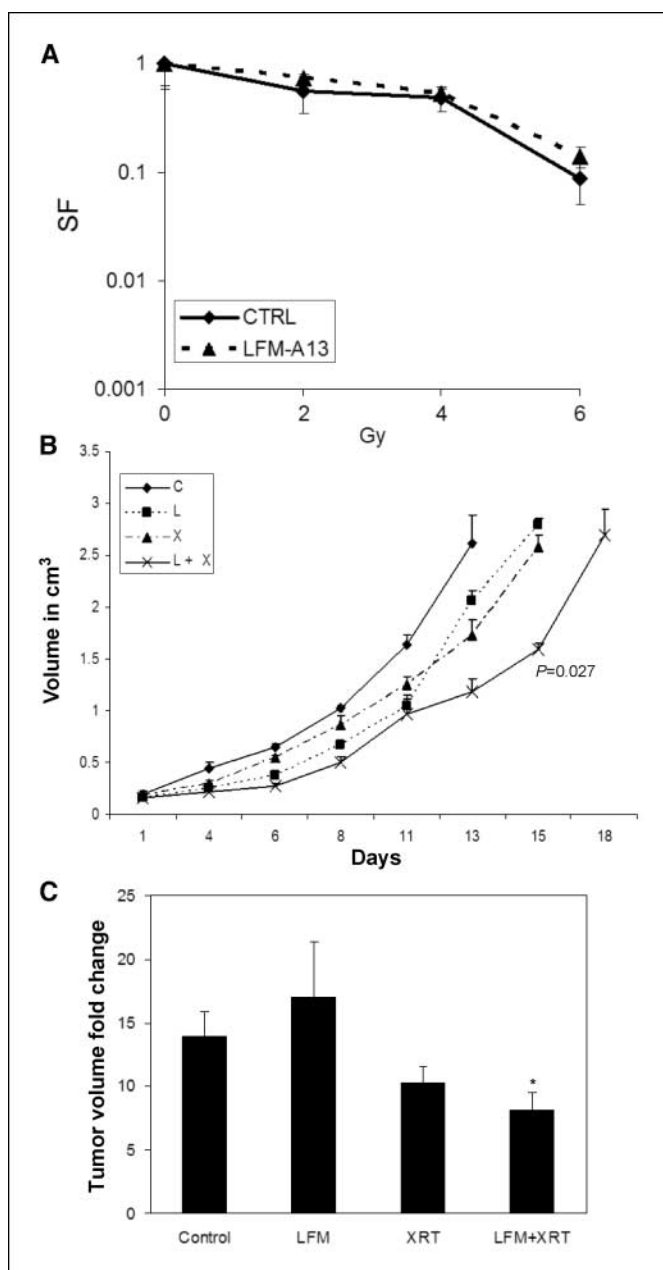


Figure 6. Bmx inhibition enhances radiation efficacy in syngeneic homograft lung cancer model. **A**, LLCs were treated with DMSO or LFM-A13 before 0, 2, 4, or 6 Gy irradiation for clonogenic survival assay as performed with HUVEC in Fig. 3. Surviving colonies were plotted as a fraction of cells plated which was normalized by the plating efficiency for each condition. *Points*, mean; *bars*, SE. **B**, LLCs were injected into the hind limb of C57BL6 mice, and tumors were allowed to form. Animals were separated into four treatment groups: DMSO vehicle control with sham irradiation (C), LFM-A13 with sham irradiation (L), radiation alone (X), or combined LFM-A13 with radiation (L+X). Treatments were given as i.p. injection of 50 mg/kg LFM-A13 45 min before 3 Gy was given daily for 5 consecutive d. Tumor size was measured and volume was calculated. *Points*, tumor volume for each group; *bars*, SE. Tumor growth delay was determined for 1.5 cm³ volume time point for each group. *P* value of 0.027 for combination treatment group. **C**, fold change in tumor volume at day 13. *, *P* < 0.05; combined arm.

The vascular effects were more pronounced in the *in vivo* tumor models. Tumor vascular window blood vessels were minimally inhibited by 2 Gy or LFM-A13 alone. However, in combination, LFM-A13 and 2 Gy substantially disrupted tumor blood vessel

formation. This antivasculature effect was confirmed in hind limb tumor models that showed that daily LFM-A13 and 3 Gy significantly affected the tumor microvasculature. Tumor growth delay was displayed in the combination arm that was more than additive.

Tec family kinase inhibition has been garnering attention, although mainly in relation to anti-inflammation. Interestingly, ImClone has developed a Bmx single chain intrabody system that can partially attenuate Src transformation potential (37). Recently, Pan et al. (38) has discovered a number of selective irreversible Btk inhibitors aimed at treating rheumatoid arthritis. Moreover, CGI Pharmaceuticals, Inc. has been developing their own novel Btk inhibitors, cgi1316 and cgi1746, for use in inflammatory diseases. However, LFM-A13, a rationally designed inhibitor developed by Parker Hughes Institute, has been extensively tested in preclinical models. The pharmacokinetics and toxicity data have been previously published (31), which provided the basis for the present study. The drug seems to be well-tolerated based on these murine studies. We have also tested another commercially available Tec family inhibitor, terreic acid (33), which seemed to be at least as effective as LFM-A13 in our *in vitro* studies (data not shown). However, because very little is known about *in vivo* toxicity and pharmacokinetics for terreic acid, we focused our study on LFM-A13.

Several lines of evidence point to Bmx as a critical player in angiogenesis, cell survival, and proliferation, particularly in response to cancer-promoting factors such as VEGF, epidermal growth factor, androgens, and Src transformation (16, 18, 25, 39–45). Bmx is activated during cellular stress such as hypoxia (17, 41, 46, 47) and plays a cytoprotective role (39–45). Bmx activation up-regulates VEGF expression in endothelial cells, and VEGF can further activate Bmx in a “feed forward” manner (17). In addition, several cancers, including prostate (48, 49) and breast (7, 50), express Bmx that is also active. Other studies show that Bmx interacts with p53 after DNA damage from chemotherapeutics in a bidirectional inhibitory manner (48). Because a predominant effect of ionizing radiation is DNA damage, this interaction may play a role in radiation sensitization by Bmx inhibitors.

Bmx provides an alternative cell survival pathway to that of PI3K-Akt signal transduction. It is possible that treatments that have targeted PI3K-Akt signaling might be deriving some of their efficacy from concomitant Bmx inhibition. Further studies are necessary to determine whether Bmx inhibition in combination with PI3K-Akt blockade will provide additional benefit. Nevertheless, Bmx inhibition remains an attractive potential target for radiation enhancement because Bmx activation occurs rapidly and transiently after radiation, such that prolonged Bmx inhibition is probably not necessary for radiation sensitization to occur. This hypothesis is consistent with our cell culture assays in which the drug was removed shortly after irradiation. Therefore, it is possible that short-acting drug formulations may be effective with radiation with less systemic effects that typically occur with long-term administration.

In summary, Bmx is a new molecular target for radiation sensitization based on *in vitro* and *in vivo* experimentation in vascular endothelium. Ongoing studies using various cancer cell lines will help us to determine whether certain cancers are more susceptible to Bmx inhibition when treated with radiation. Ultimately, clinical evaluation of Bmx inhibitors with radiation

will be critical during the development of Bmx as a biological target for therapy.

Acknowledgments

Received 10/3/2007; revised 1/22/2008; accepted 2/14/2008.

References

- Valerie K, Yacoub A, Hagan MP, et al. Radiation-induced cell signaling: inside-out and outside-in. *Mol Cancer Ther* 2007;6:789–801.
- Sonveaux P, Frerart F, Bouzin C, et al. Irradiation promotes Akt-targeting therapeutic gene delivery to the tumor vasculature. *Int J Radiat Oncol Biol Phys* 2007;67:1155–62.
- Zingg D, Riesterer O, Fabbro D, Glanzmann C, Bodis S, Pruschy M. Differential activation of the phosphatidylinositol 3'-kinase/Akt survival pathway by ionizing radiation in tumor and primary endothelial cells. *Cancer Res* 2004;64:5398–406.
- Tan J, Geng L, Yazlovitskaya EM, Hallahan DE. Protein kinase B/Akt-dependent phosphorylation of glycogen synthase kinase-3 β in irradiated vascular endothelium. *Cancer Res* 2006;66:2320–7.
- Tan J, Hallahan DE. Growth factor-independent activation of protein kinase B contributes to the inherent resistance of vascular endothelium to radiation-induced apoptotic response. *Cancer Res* 2003;63:7663–7.
- Chan TO, Rittenhouse SE, Tschlis PN. AKT/PKB and other D3 phosphoinositide-regulated kinases: kinase activation by phosphoinositide-dependent phosphorylation. *Annu Rev Biochem* 1999;68:965–1014.
- Chen R, Kim O, Li M, et al. Regulation of the PH-domain-containing tyrosine kinase Etk by focal adhesion kinase through the FERM domain. *Nat Cell Biol* 2001;3:439–44.
- Nore BF, Mattsson PT, Antonsson P, et al. Identification of phosphorylation sites within the SH3 domains of Tec family tyrosine kinases. *Biochim Biophys Acta* 2003;1645:123–32.
- Pan S, An P, Zhang R, He X, Yin G, Min W. Etk/Bmx as a tumor necrosis factor receptor type 2-specific kinase: role in endothelial cell migration and angiogenesis. *Mol Cell Biol* 2002;22:7512–23.
- Qiu Y, Kung HJ. Signaling network of the Btk family kinases. *Oncogene* 2000;19:5651–61.
- Smith CI, Islam TC, Mattsson PT, Mohamed AJ, Nore BF, Vihinen M. The Tec family of cytoplasmic tyrosine kinases: mammalian Btk, Bmx, Itk, Tec, and homologs in other species. *Bioessays* 2001;23:436–46.
- Vargas L, Nore BF, Berglof A, et al. Functional interaction of caveolin-1 with Bruton's tyrosine kinase and Bmx. *J Biol Chem* 2002;277:9351–7.
- Yang J, Kim O, Wu J, Qiu Y. Interaction between tyrosine kinase Etk and a RUN domain- and FYVE domain-containing protein RUFY1. A possible role of ETK in regulation of vesicle trafficking. *J Biol Chem* 2002;277:30219–26.
- Kaukonen J, Lahtinen I, Laine S, Alitalo K, Palotie A. Bmx tyrosine kinase gene is expressed in granulocytes and myeloid leukaemias. *Br J Haematol* 1996;94:455–60.
- Mano H. Tec family of protein-tyrosine kinases: an overview of their structure and function. *Cytokine Growth Factor Rev* 1999;10:267–80.
- Wen X, Lin HH, Shih HM, Kung HJ, Ann DK. Kinase activation of the non-receptor tyrosine kinase Etk/BMX alone is sufficient to transactivate STAT-mediated gene expression in salivary and lung epithelial cells. *J Biol Chem* 1999;274:38204–10.
- Chau CH, Clavijo CA, Deng HT, et al. Etk/Bmx mediates expression of stress-induced adaptive genes VEGF, PAI-1, and iNOS via multiple signaling cascades in different cell systems. *Am J Physiol Cell Physiol* 2005;289:C444–54.
- Chau CH, Chen KY, Deng HT, et al. Coordinating Etk/Bmx activation and VEGF upregulation to promote cell survival and proliferation. *Oncogene* 2002;21:8817–29.
- Zhang R, Xu Y, Ekman N, et al. Etk/Bmx transactivates vascular endothelial growth factor 2 and recruits phosphatidylinositol 3-kinase to mediate the tumor necrosis factor-induced angiogenic pathway. *J Biol Chem* 2003;278:51267–76.
- Ekman N, Arighi E, Rajantie I, et al. The Bmx tyrosine kinase is activated by IL-3 and G-CSF in a PI-3K dependent manner. *Oncogene* 2000;19:4151–8.
- Qiu Y, Robinson D, Pretlow TG, Kung HJ. Etk/Bmx, a tyrosine kinase with a pleckstrin-homology domain, is an effector of phosphatidylinositol 3'-kinase and is involved in interleukin 6-induced neuroendocrine differentiation of prostate cancer cells. *Proc Natl Acad Sci U S A* 1998;95:3644–9.
- Cote JF, Motoyama AB, Bush JA, Vuori K. A novel and evolutionarily conserved PtdIns(3,4,5)P₃-binding domain is necessary for DOCK180 signalling. *Nat Cell Biol* 2005;7:797–807.
- Kim O, Yang J, Qiu Y. Selective activation of small GTPase RhoA by tyrosine kinase Etk through its pleckstrin homology domain. *J Biol Chem* 2002;277:30066–71.
- Lee LF, Guan J, Qiu Y, Kung HJ. Neuropeptide-induced androgen independence in prostate cancer cells: roles of nonreceptor tyrosine kinases Etk/Bmx, Src, and focal adhesion kinase. *Mol Cell Biol* 2001;21:8385–97.
- Abassi YA, Rehn M, Ekman N, Alitalo K, Vuori K. p130Cas Couples the tyrosine kinase Bmx/Etk with regulation of the actin cytoskeleton and cell migration. *J Biol Chem* 2003;278:35636–43.
- Jui HY, Tseng RJ, Wen X, et al. Protein-tyrosine phosphatase D1, a potential regulator and effector for Tec family kinases. *J Biol Chem* 2000;275:41124–32.
- Tomlinson MG, Heath VL, Turck CW, Watson SP, Weiss A. SHIP family inositol phosphatases interact with and negatively regulate the Tec tyrosine kinase. *J Biol Chem* 2004;279:55089–96.
- Cuneo KC, Tu T, Geng L, Fu A, Hallahan DE, Willey CD. HIV protease inhibitors enhance the efficacy of irradiation. *Cancer Res* 2007;67:4886–93.
- Edwards E, Geng L, Tan J, Onishko H, Donnelly E, Hallahan DE. Phosphatidylinositol 3-kinase/Akt signaling in the response of vascular endothelium to ionizing radiation. *Cancer Res* 2002;62:4671–7.
- He H, Hirokawa Y, Gazit A, et al. The Tyr-kinase inhibitor AG879, that blocks the ETK-PAK1 interaction, suppresses the RAS-induced PAK1 activation and malignant transformation. *Cancer Biol Ther* 2004;3:96–101.
- Uckun FM, Zheng Y, Cetkovic-Cvrlje M, et al. *In vivo* pharmacokinetic features, toxicity profile, and chemosensitizing activity of α -cyano- β -hydroxy- β -methyl-N-(2,5-dibromophenyl)propanamide (LFM-A13), a novel antileukemic agent targeting Bruton's tyrosine kinase. *Clin Cancer Res* 2002;8:1224–33.
- Mahajan S, Ghosh S, Sudbeck EA, et al. Rational design and synthesis of a novel anti-leukemic agent targeting Bruton's tyrosine kinase (BTK), LFM-A13 [α -cyano- β -hydroxy- β -methyl-N-(2,5-dibromophenyl)propanamide]. *J Biol Chem* 1999;274:9587–99.
- Kawakami Y, Hartman SE, Kinoshita E, et al. Terreic acid, a quinone epoxide inhibitor of Bruton's tyrosine kinase. *Proc Natl Acad Sci U S A* 1999;96:2227–32.
- Geng L, Tan J, Himmelfarb E, et al. A specific antagonist of the p110 δ catalytic component of phosphatidylinositol 3'-kinase, IC486068, enhances radiation-induced tumor vascular destruction. *Cancer Res* 2004;64:4893–9.
- Lee CM, Fuhrman CB, Planelles V, et al. Phosphatidylinositol 3-kinase inhibition by LY294002 radiosensitizes human cervical cancer cell lines. *Clin Cancer Res* 2006;12:250–6.
- Lu B, Shinohara ET, Edwards E, Geng L, Tan J, Hallahan DE. The use of tyrosine kinase inhibitors in modifying the response of tumor microvasculature to radiotherapy. *Technol Cancer Res Treat* 2005;4:691–8.
- Paz K, Brennan LA, Iacolina M, Doody J, Hadari YR, Zhu Z. Human single-domain neutralizing intrabodies directed against Etk kinase: a novel approach to impair cellular transformation. *Mol Cancer Ther* 2005;4:1801–9.
- Pan Z, Scheerens H, Li SJ, et al. Discovery of Selective Irreversible Inhibitors for Bruton's Tyrosine Kinase. *ChemMedChem* 2007;2:58–61.
- Tsai YT, Su YH, Fang SS, et al. Etk, a Btk family tyrosine kinase, mediates cellular transformation by linking Src to STAT3 activation. *Mol Cell Biol* 2000;20:2043–54.
- Saharinen P, Ekman N, Sarvas K, Parker P, Alitalo K, Silvennoinen O. The Bmx tyrosine kinase induces activation of the Stat signaling pathway, which is specifically inhibited by protein kinase C δ . *Blood* 1997;90:4341–53.
- Zhang J, Ping P, Wang GW, et al. Bmx, a member of the Tec family of nonreceptor tyrosine kinases, is a novel participant in pharmacological cardioprotection. *Am J Physiol Heart Circ Physiol* 2004;287:H2364–6.
- Xie Y, Xu K, Dai B, et al. The 44 kDa Pim-1 kinase directly interacts with tyrosine kinase Etk/BMX and protects human prostate cancer cells from apoptosis induced by chemotherapeutic drugs. *Oncogene* 2006;25:70–8.
- Xue LY, Qiu Y, He J, Kung HJ, Oleinick NL. Etk/Bmx, a PH-domain containing tyrosine kinase, protects prostate cancer cells from apoptosis induced by photodynamic therapy or thapsigargin. *Oncogene* 1999;18:3391–8.
- Stoletov KV, Terman BI. Bmx is a downstream Rap1 effector in VEGF-induced endothelial cell activation. *Biochem Biophys Res Commun* 2004;320:70–5.
- Paavonen K, Ekman N, Wirzenius M, Rajantie I, Poutanen M, Alitalo K. Bmx tyrosine kinase transgene induces skin hyperplasia, inflammatory angiogenesis, and accelerated wound healing. *Mol Biol Cell* 2004;15:4226–33.
- Mathur P, Kaga S, Zhan L, Das DK, Maulik N. Potential candidates for ischemic preconditioning-associated vascular growth pathways revealed by antibody array. *Am J Physiol Heart Circ Physiol* 2005;288:H3006–10.
- Rajantie I, Ekman N, Iljin K, et al. Bmx tyrosine kinase has a redundant function downstream of angiopoietin and vascular endothelial growth factor receptors in arterial endothelium. *Mol Cell Biol* 2001;21:4647–55.
- Jiang T, Guo Z, Dai B, et al. Bi-directional regulation between tyrosine kinase Etk/BMX and tumor suppressor p53 in response to DNA damage. *J Biol Chem* 2004;279:50181–9.
- Dai B, Kim O, Xie Y, et al. Tyrosine kinase Etk/BMX is up-regulated in human prostate cancer and its overexpression induces prostate intraepithelial neoplasia in mouse. *Cancer Res* 2006;66:8058–64.
- Bagheri-Yarmand R, Mandal M, Taludker AH, et al. Etk/Bmx tyrosine kinase activates Pak1 and regulates tumorigenicity of breast cancer cells. *J Biol Chem* 2001;276:29403–9.